NBSIR 83-2765

Calculations of Wall Fire Spread in an Enclosure

U.S. DEPARTMENT OF COMMERCE
National Bureau of Standards
National Engineering Laboratory
Center for Fire Research
Washington, D.C. 20234

November 1983

NBSIR 83-2765

CALCULATIONS OF WALL FIRE SPREAD IN AN ENCLOSURE

Kenneth D. Steckler

TABLE OF CONTENTS

.

LIST OF FIGURES

LIST OF TABLES

a_j — wall properties parameter (equation 4-11), s^{-1}

A_b — total burning wall area, m^2

A'_b — burning area on adjacent wall, m^2

A_c — area of crib exposed to external radiation, m^2

A_F — area of floor, m^2

A_i — internal area of crib(s), m^2

A_{ou} — area of room opening in upper layer, m^2

A_{wu} — enclosure surface area bounding upper layer, m^2

A_{wl} — enclosure surface area bounding lower layer, m^2

A_{inv} — area of involvement, $(A_b + A_{py})$, m^2

A_{py} — pyrolyzing wall area, m^2

C $\begin{cases} - \text{ empirical material constant (equations 7-7 and 7-8), } m^{3/2} s^{1/2}/kW \\ - \text{ radial function in equation A-11a} \end{cases}$

C_i — opening flow coefficient (inflow)

C_o — opening flow coefficient (outflow)

c_p — specific heat of air, J/g-K

c_{pp} — specific heat of pyrolysis gases, J/g-K

c_{pw} — specific heat of enclosure walls, ceiling, and floor, J/g-K

D — distance between area elements on adjacent walls (Appendix C), m

$\dot{E}''$ — energy release rate per unit area, kW/m^2

$\dot{E}_L$ — rate of energy transfer by heat transport, kW

$\dot{E}_M$ — rate of energy transfer by mass transport, kW

$\dot{E}_R$ — energy release rate, kW

f — fraction of total energy release radiated by flame

f_1
f_2
f_3
f_4 — governing equations in model
f_5
f_6
f_7

$F_{dA,i}$
      — radiative exchange geometrical factors
$F_{r,s}$

g — gravitational acceleration, m/s^2

H — room height, m

H_o — opening heights, m

ΔH — heat of combustion, kJ/kg

h_c — convective heat transfer coefficient, kW/m^2-K

k — number of horizontal strips into which wall is divided (figure 7-1)

k_f — flame attenuation coefficient, m^{-1}

k_g — upper layer attenuation coefficient, m^{-1}

k_m — mixing coefficient

k_w — thermal conductivity of walls, ceiling, and floor, kW/m-K

L — room length, m

L_m — mean beam length based on entire upper layer volume, m

$L_{m,i}$ — mean beam length based on portion of upper layer volume, m

L_{vap} — effective heat of vaporization of fuel, kJ/kg

ℓ_f — flame thickness, m

ℓ_g — path length through upper layer (Appendix C), m

m — flame spread parameter (equations 7-8)

$\dot{m}_b$ — burning rate, kg/s

$\dot{m}_b''$ — burning rate per unit area, kg/m^2-s

$\dot{m}''_{b;w,k,i}$ — local burning rate per unit area (figure 7-1), kg/m^2-s

$\dot{m}''_{b,crit}$ — critical fuel supply rate per unit area necessary to sustain burning, kg/m^2-s

$\dot{m}_e$ — mixing mass flow rate from upper to lower gas layer, kg/s

$\dot{m}_i$ — mass flow rate through opening into room, kg/s

$\dot{m}_o$ — mass flow rate through opening from room, kg/s

$\dot{m}_{in}$ — mass flow rate to layer, kg/s

$\dot{m}_{out}$ — mass flow rate from layer, kg/s

$\dot{m}_v$ — pyrolysis rate, kg/s

$\dot{m}_p$ — entrainment rate of gas into flame and plume, kg/s

$\dot{m}_v$ — fuel pyrolysis rate, kg/s

$\dot{m}''_v$ — fuel pyrolysis rate per unit area, kg/m^2-s

$\dot{m}''_{v;w,k,i}$ — local pyrolysis rate per unit area (figure 7-1), kg/m^2-s

$\dot{m}_{vo}$ — free-burn pyrolysis rate, kg/s

$\dot{m}''_{vo}$ — free-burn fuel pyrolysis rate per unit area, kg/m^2-s

N — number of slabs in finite-difference wall

p — pressure, N/m^2

Q — rate of energy release by fire (equation 7-17), kW

Q^* — dimensionless rate of energy release

$\dot{q}''_f$ — incident radiant flux from flaming areas of adjacent wall, kW/m^2

$\dot{q}''_e$ — radiant flux emitted per unit area of flaming material (equation 7-14)

$\dot{q}''_i$ — incident radiant flux, kW/m^2

$\dot{q}''_i{}^*$ — minimum external radiant flux necessary to sustain burning at reference state, kW/m^2

$\dot{q}''_i{}^{**}$ — minimum external flux to cause mass loss, kW/m^2

$\dot{q}''_{i,ig}$ — minimum flux necessary for piloted ignition, kW/m^2

$\dot{q}''_c$ — heat flux convected to surface, kW/m^2

$\dot{q}''_{gw}$ — incident radiant flux from enclosure surfaces and upper gas layer, kW/m^2

$\dot{q}''_k$ — heat flux conducted into surface, kW/m^2

$\dot{q}''_{rc}$ — external radiant flux incident upon crib, kW/m^2

$\dot{q}''_{rd}$ — net flux radiated through layer interface from upper to lower spaces, kW/m^2

$\dot{q}''_{rl}$ — net flux radiated to lower surfaces of enclosure, kW/m^2

$\dot{q}''_{ro}$ — net flux radiated from upper layer through room opening, kW/m^2

$\dot{q}''_{ru}$ — net flux radiated to upper surfaces of enclosure, kW/m^2

$\dot{q}''_w$ — net flux to exposed enclosure surface, kW/m^2

$\dot{q}''_{wo}$ — net flux from unexposed enclosure surface, kW/m^2

r — stoichiometric air-to-fuel mass ratio
{
— characteristic radius (equation A-11a), m

t — time, s

Δt — time increment, s

t^* — characteristic burn time, s

T — temperature of gas or wall, $^{\circ}$C or K

T_1 — temperature of exposed surface of finite difference slab, $^{\circ}$C or K

T_2 — temperature of unexposed surface of finite difference slab, $^{\circ}$C or K

T_a — ambient temperature, $^{\circ}$C or K

T_f — flame temperature, K

T_{gl} — lower gas layer temperature, $^{\circ}$C or K

T_{gu} — upper gas layer temperature, $^{\circ}$C or K

T_j — finite difference wall slab temperature, $^{\circ}$C or K

T_s — temperature of surface behind flames, (equations 7-15 and A-6) ,K

T_w — temperature of enclosure exposed surface, $^{\circ}$C or K

T_{∞} — reference temperature for ideal gas calculation, $^{\circ}$C or K

T_{wj} -- either T_{wu} or T_{wl} (equation 7-17), $^{\circ}C$ or K

v_f -- flame spread rate, m/s

$v_{w,k,i}$ -- local horizontal flame spread rate (figure 7-1), m/s

v_{∞} -- limiting flame spread rate, m/s

W -- room width, m

W_o -- opening width, m

x -- position coordinate (Appendices B and C), m

$x_{w,k,i}$ -- horizontal coordinate used in wall spread calculation (figure 7-1), m

X $\begin{cases} - \text{ depth coordinate within wall (equation 4-7), m} \\ - \text{ dummy variable (equations B-6 and B-7a)} \end{cases}$

X_a -- ratio of excess air after combustion to air required by combustion

ΔX -- wall thickness increment, m

y -- position coordinate (Appendix C), m

Y -- dummy variable (Appendix C)

Y_{ox} -- oxygen mass fraction

Y_{oxl} -- oxygen mass fraction in lower layer

Y_{oxu} -- oxygen mass fraction in upper layer

$Y_{ox,crit}$ -- critical oxygen concentration below which burning ceases

Y_{ox}^{*} -- oxygen mass fraction; reference state

Z -- height coordinate, m

$Z_{w,k,i}$ -- vertical coordinate used in wall spread calculation (figure 7-1), m

ΔZ -- height increment, m

Z_d -- thermal discontinuity height, m

Z_e -- entrainment height, m

Z_n -- neutral plane height, m

z_1 —   vertical wall coordinate (Appendix C), m

z_2 —   vertical wall coordinate (Appendix C), m

δ_i —   horizontal dimension of initial flaming area, m

δ_w —   wall thickness, m

ϵ_g —   average emissivity of upper gas layer

$\epsilon_{g,i}$ —   average emissivity of gas within a portion of upper layer (equation 7-9)

ϵ_s —   emissivity of surface behind flame (equation 7-14)

ξ —   burning-rate parameter (equation 7-2), kg/m^2-s

γ_1 —   area ratio (equation A-17a)

γ_u —   area ratio (equation A-8a)

ρ —   density of gas, kg/m^3

ρ_a —   density of air at ambient temperature, kg/m^3

ρ_w —   density of walls, ceiling and floor, kg/m^3

ρ_∞ —   density of air at reference temperature, T_∞, kg/m^3

σ —   Stefan-Boltzman constant (5.67×10^{-11} kW/m^2-K^4)

Calculations of Wall Fire Spread in an Enclosure

Kenneth D. Steckler

Center for Fire Research
National Engineering Laboratory
National Bureau of Standards
Washington, D.C. 20234

Abstract

Mathematical models of fire growth in enclosures offer a
potential for assessing the risk of materials with respect to a
hazard such as flashover. The development of a model for fire
spread over wall lining materials is presented. The work covers
the development of a transient two-layer zone model, initially
formulated for crib fires in a room, then adapted to simulate a
spreading corner wall fire. The local wall flame spread rate and
burning rate per unit area are expressed in the model as functions
of the external radiation incident upon the burning surface and
the oxygen concentration in the adjacent gas layer (zone). Flame
spread is limited to the horizontal direction. Results for a
fictitious wall lining material are presented. Major elements of
the results are shown to be in qualitative agreement with
experience. Finally, areas for improvement and the direction of
future efforts are noted.

Key words: burning rate; fire models; flame spread; flashover;
hazard assessment; interior finishes; room fires; walls.

1. INTRODUCTION

A common room-fire scenario involves the ignition of an object such as a
wastebasket positioned near a combustible wall surface, ignition of the wall
lining material, and subsequent fire spread on the wall lining. In many cases
the energy released by the wastebasket alone would be insufficient to produce
a dangerous environment within the room. However, when the wastebasket is
located near a wall in a room, whether the fire continues to grow to a

hazardous condition such as flashover, or merely burns out, depends on the fire characteristics of the lining material and the extent to which the enclosure dissipates the energy and combustion products released by the burning material. With knowledge of a characteristic energy release rate per unit area, $\dot{E}''$, and the flame spread rate, v_f, of the burning wall lining material, an evaluation of the potential hazard of flashover should be possible. If an evaluation of potential hazard due to development of a toxic atmosphere is desired, then knowledge of the rates of production of hazardous species per unit area would also be required.

In a qualitative sense, one would expect a flashover "hazard index" for a lining material to include some combination of v_f and $\dot{E}''$ to reflect the total energy release rate of the material. Unfortunately, "combining" v_f and $\dot{E}''$ is complicated by the fact that both parameters tend to be functions (at least) of exposure conditions such as incident radiant flux and oxygen concentration [1-6]. When a material burns within an enclosure, portions of the energy and combustion products released by the fire accumulate within the enclosure and portions feed back to the burning material. Therefore, $\dot{E}''$ and v_f are coupled through the properties of the overall enclosure. A more detailed analysis of the interactions between the burning lining material and enclosure is required to assess the roles of $\dot{E}''$ and v_f in contributing to the hazard of flashover. The required analysis is mathematical modeling.

Mathematical models of fire growth in enclosures represent assemblages of mathematical expressions which describe in varying degrees the complex physical interactions between a burning material and its environment. One class of models, known as zone or control volume models [7-12], treats the developing room fire in terms of several volume and boundary elements which intercommunicate energy and/or mass. Conservation equations are written for each zone and solved using a numerical technique. Applying such models leads to solutions for the state variables of each zone and the various interzonal mass and energy transfers.

Several zone models treat fires which grow in area. Emmons and Mitler [8] and Rockett [13] modeled fire spread on a horizontal (mattress) surface within an enclosure while McArthur and Meyer [10] treated the case of fire

2

spread on seats and walls in an aircraft cabin. Tanaka [14] and Smith [11] modeled the developing wall fire in a room. The current work follows an approach suggested by Quintiere [15]. It differs from the earlier work in that the different oxygen concentrations in the upper and lower gas layers within the enclosure are taken into account in predicting the burning and flame spread rates in these layers.

The objective is to formulate and execute a "first-cut" mathematical zone model which handles enough of the phenomena depicted in figure 1-1 so as to 1) produce results which are qualitatively reasonable and 2) provide a basis for a more complete model which will provide an answer to the question: If a given wall lining is ignited, will the room reach flashover conditions? It was judged that a model having the following limited features would lead to this objective and be tractable within the time allocated for the project.

a. The wall lining is the only combustible material in the room.

b. Only the fire spread, not ignition, is considered. This assumes that a portion of wall-corner area is already burning and that the ignition source is either no longer present or is insignificant.

c. Flames are restricted to the wall areas; that is, there are no flame extensions on the ceiling.

d. As a first approximation flame spread is restricted to the horizontal direction.

e. Burning rates per unit area and flame spread rates are expressed as functions of the oxygen concentration of the gas layer (upper or lower) in which the area element is located and of the local incident external radiant flux. This approach is motivated by the existence of experimental results and theoretical analyses for steady or mean time burning and flame spread rates as a function of external oxygen concentration and heat flux. Therefore local burning and flame spread rates will be assumed to instantaneously take on steady values consistent with the instantaneous values of the time-dependent

3

external heat flux and oxygen concentration. This leads to a conservative estimate of these rates and avoids the problem of calculating local wall temperature histories. As a further simplification, it will be assumed that the external heat flux which drives the burning and flame spread rates is solely radiative: that is, these rates are independent of convective effects from the gas zone or layer in which the material is immersed.

f.   The flame spread model assumes countercurrent gas flow in all locations. The one place where this clearly does not bear out is the ceiling jet region.

g.   The room conditions and interactions between the room and burning material are formulated as a transient version of the quasi-steady room fire model of Quintiere and McCaffrey [12].

2.   APPROACH

The approach used to develop the corner wall spread model is diagrammed in figure 2-1. Transient features such as gas layer transients, wall heat conduction*, and time-dependent energy release of the fire source were added to the quasi-steady model for crib fires in an enclosure [12]. Actually two transient enclosure fire models are developed in the following sections; one for a time-dependent crib source and the other for a spreading wall fire source. The transient crib model provided a convenient means for evaluating the transient conduction and gas layer sub-models before proceeding with the more complicated wall-spread source.

---

*With respect to heat transfer by conduction, the ceiling and floor are treated as extensions of the upper and lower wall surfaces, respectively. Therefore, "wall conduction" refers to either wall and ceiling or wall and floor heat conduction.

4

3. DESCRIPTION OF QUASI-STEADY MODEL

The quasi-steady model, which served as the starting point for this project, will be briefly described in this section. Basically the model predicts the quasi-steady conditions within an enclosure, including the burning rate of the crib(s), given the free-burn rate of the crib(s) and other properties of the enclosure. A more detailed description can be found in the literature [12].

The model casts the enclosure fire in terms of control volumes or zones, and the physical boundaries of these zones (figure 3-1). Mass and energy balances are written for each zone and boundary as functions of seven independent variables; namely,

Z_n — height of neutral plane in the opening,

Z_d — height of thermal discontinuity within the room,

T_{gu} — temperature of gas in upper layer,

T_{gl} — temperature of gas in lower layer,

T_{wu} — temperature of wall and ceiling bounding upper gas layer,

T_{wl} — temperature of wall and floor bounding lower gas layer, and

$\dot{m}_v$ — fuel pyrolysis rate.

This produces seven simultaneous non-linear algebraic equations of the form

$$f_1(Z_n, Z_d, T_{gu}, T_{gl}, T_{wu}, T_{wl}, \dot{m}_v) = 0$$
$$f_2(Z_n, Z_d, T_{gu}, T_{gl}, \dot{m}_v) = 0$$
$$f_3(Z_n, Z_d, T_{gu}, T_{gl}, T_{wu}, T_{wl}, \dot{m}_v) = 0$$
$$f_4(Z_n, Z_d, T_{gu}, T_{gl}) = 0 \qquad (3\text{-}1)$$
$$f_5(Z_n, Z_d, T_{gu}, T_{gl}, T_{wu}, T_{wl}, \dot{m}_v) = 0$$
$$f_6(Z_n, Z_d, T_{gu}, T_{gl}, T_{wu}, T_{wl}, \dot{m}_v) = 0$$
$$f_7(Z_n, Z_d, T_{gu}, T_{gl}, T_{wu}, T_{wl}, \dot{m}_v) = 0$$

which must be solved by numerical methods.

Specifically, the seven equations describe the following quasi-steady processes:

a. Mass balance for the enclosure:

$$f_1 = \dot{m}_o - \dot{m}_i - \dot{m}_v = 0 \tag{3-2}$$

      where $\dot{m}_o$ is the mass flow rate outward through the room opening (equation A-1 listed in Appendix A),

                $\dot{m}_i$ is the inward mass flow rate through the opening (equation A-2),

                $\dot{m}_v$ is the fuel pyrolysis rate (see equation 3-8).

b. Mass balance for lower gas layer:

$$f_2 = \dot{m}_p - \dot{m}_i - \dot{m}_e = 0 \tag{3-3}$$

      where $\dot{m}_p$ is entrainment rate into the crib and plume (equation A-3),

                $\dot{m}_e$ is the mass flow rate from the upper to lower layer due to entrainment (mixing) at the opening (equation A-4).

c. Upper gas layer energy balance:

$$f_3 = \dot{E}_{Ru} - \dot{E}_{Lu} - \dot{E}_{Mu} = 0 \tag{3-4}$$

      where $\dot{E}_{Ru}$ is the rate at which energy is released in the layer (equation A-5), (note: in figure 3-1 the crib is located in the upper layer),

6

$\dot{E}_{Lu}$ is the net rate of energy loss from the layer by heat transfer (equation A-7)

$\dot{E}_{Mu}$ is the net rate of energy loss due to mass transfer (equation A-6).

d. Lower layer energy balance:

$$f_4 = \dot{E}_{M1} + \dot{E}_{L1} = 0 \qquad (3-5)$$

where $\dot{E}_{M1}$ is the net rate of energy loss by mass transfer (equation A-12),

$\dot{E}_{L1}$ is the net rate of energy loss by heat transfer when the gas is not considered to be absorbing or emitting (equation A-13).

e. Energy balance at upper gas-wall interface:

$$f_5 = \dot{q}''_{ku} - \dot{q}''_{ru} - \dot{q}''_{cu} = 0 \qquad (3-6)$$

where $\dot{q}''_{ku}$ is the heat flux conducted from the surface into the upper wall (equation A-14),

$\dot{q}''_{ru}$ is the net radiative flux to the upper wall surface (equation A-8),

$\dot{q}''_{cu}$ is the flux convected from the gas to the upper wall surface (equation A-11).

f. Energy balance at lower gas-wall interface:

$$f_6 = \dot{q}''_{k1} - \dot{q}''_{r1} - \dot{q}''_{c1} = 0 \qquad (3-7)$$

7

where $\dot{q}''_{kl}$ is the heat flux conducted from the surface into the lower wall (equation A-15),

$\dot{q}''_{rl}$ is the net radiative flux to the lower wall surface (equation A-17),

$\dot{q}''_{cl}$ is the convected flux from the gas to the lower wall surface (equation A-16).

g. Fuel pyrolysis rate

$$f_7 = \dot{m}_v - \dot{m}''_{vo} A_i (Y_{oxl}/0.23) - (\dot{q}''_{rc} A_c / L_{vap}) = 0 \qquad (3-8)$$

where $\dot{m}_v$ is the fuel pyrolysis rate,

$\dot{m}''_{vo}$ is the peak free-burn pyrolysis rate per unit area,

A_i is the internal area of the crib,

A_c is the area of crib exposed to external radiation,

$\dot{q}''_{rc}$ is the external radiant flux incident upon crib,

Y_{oxl} is the mass fraction of oxygen in the lower layer (equation A-18),

L_{vap} is the fuel's effective heat of vaporization.

The burning rate, $\dot{m}_b$, is defined in equation A-3 as the smaller of $\dot{m}_v$ (fuel controlled) and m_i/r (ventilation controlled), where r is the stoichiometric air-to-(volatilized) fuel mass ratio. The model also computes the mass fraction of oxygen in the upper layer, Y_{oxu} (equation A-19).

8

4. DEVELOPMENT OF GAS LAYER AND WALL CONDUCTION EQUATIONS FOR A TRANSIENT TWO-LAYER MODEL

The equations presented in section 3 for the conservation of mass and energy in the two gas layers (equations 3-2 to 3-5) are based on the assumption that the time derivative or transient terms of the more complete equations are negligible with respect to the retained terms. This is a good assumption for near-steady conditions, but could lead to significant errors if the early stages of fire growth were modeled as a sequence of quasi-steady states. Similarly, the quasi-steady wall conduction terms, $\dot{q}''_{ku}$ and $\dot{q}''_{kl}$, in gas-wall interface equations 3-6 and 3-7, could produce comparable errors in such an analysis. Therefore, more complete equations for mass and energy conservation are needed to address the spreading wall fire problem.

4.1 Transient Equations for Conservation of Mass and Energy in a Gas Layer

Following the analysis of Quintiere [15], the equation of continuity for a generic uniform gas layer shown in figure 4-1 is

$$WL \frac{d}{dt} (\rho Z) + \dot{m}_{out} - \dot{m}_{in} = 0. \tag{4-1}$$

The first term accounts for changes in the layer thickness, Z, and layer density, ρ, with time, t. The second and third terms represent the mass flow to and from the layer, respectively. A transient energy equation for the same layer is given by the expression

$$WLZ \frac{dp}{dt} - WLZ\rho c_p \frac{dT}{dt} + \dot{E}_R - \dot{E}_L - \dot{E}_M = 0 \tag{4-2}$$

where the first term accounts for energy used to change the total pressure within the layer, the second term accounts for energy used to change the temperature of the layer, $\dot{E}_R$ is the rate of energy release within the layer, $\dot{E}_L$ is the rate of energy loss by heat transfer, and $\dot{E}_M$ is the rate of energy loss by mass transfer.

In applying equation 4-2 to residential room fires of the type shown in figures 1-1 and 2-1, it appears reasonable to assume that the total pressure, p, remains nearly constant [15]. Therefore, the dp/dt term can be ignored. If time derivatives are expressed as simple forward finite differences, the resulting set of conservation equations for the upper and lower gas layers is

a. Mass (upper plus lower layers):

$$f_1 = WL\rho_\infty T_\infty \left\{ \left[\frac{1}{T_{gl}(t)} - \frac{1}{T_{gu}(t)} \right] \frac{Z_d(t + \Delta t) - Z_d(t)}{\Delta t} - \frac{Z_d(t)}{T_{gl}^2(t)} \cdot \right.$$

$$\left. \frac{T_{gl}(t + \Delta t) - T_{gl}(t)}{\Delta t} - \frac{H - Z_d(t)}{T_{gu}^2(t)} \frac{T_{gu}(t + \Delta t) - T_{gu}(t)}{\Delta t} \right\} \quad (4\text{-}3)$$

$$+ \dot{m}_o(t + \Delta t) - \dot{m}_1(t + \Delta t) - \dot{m}_v(t + \Delta t) = 0$$

b. Mass (lower layer):

$$f_2 = WL\rho_\infty T_\infty \left\{ \frac{1}{T_{gl}(t)} \frac{Z_d(t + \Delta t) - Z_d(t)}{\Delta t} - \frac{Z_d(t)}{T_{gl}^2(t)} \frac{T_{gl}(t + \Delta t) - T_{gl}(t)}{\Delta t} \right\}$$

$$(4\text{-}4)$$

$$+ \dot{m}_p(t + \Delta t) - \dot{m}_1(t + \Delta t) - \dot{m}_e(t + \Delta t) = 0$$

c. Energy (upper layer):

$$f_3 = -WL\rho_\infty T_\infty c_p \frac{H - Z_d(t)}{T_{gu}(t)} \frac{T_{gu}(t + \Delta t) - T_{gu}(t)}{\Delta t}$$

$$(4\text{-}5)$$

$$+ \dot{E}_{Ru}(t + \Delta t) - \dot{E}_{Lu}(t + \Delta t) - \dot{E}_{Mu}(t + \Delta t) = 0$$

d. Energy (lower layer):

$$f_4 = WL\rho_\infty T_\infty c_p \frac{Z_d(t)}{T_{gl}(t)} \frac{T_{gl}(t + \Delta t) - T_{gl}(t)}{\Delta t}$$

$$(4\text{-}6)$$

$$+ \dot{E}_{Ml}(t + \Delta t) + \dot{E}_{Ll}(t + \Delta t) = 0$$

where $\dot{m}_o$, $\dot{m}_i$, $\dot{E}_{Ru}$, etc. are obtained from the subsidiary equations in Appendix A using $Z_n(t + \Delta t)$, $Z_d(t + \Delta t)$, $T_{gu}(t + \Delta t)$, etc. If Z_d, T_{gu}, and T_{g1} are independent of time, the above equations reduce to quasi-steady equations 2-2 to 2-5.

4.2 Transient Wall Conduction Equations

Heat conduction through the walls of the enclosure will be treated as a one-dimensional process. A solution to the transient heat conduction equation

$$\frac{\partial}{\partial X} \ k_w(T) \ \frac{\partial T(X,t)}{\partial X} = \rho_w \ c_{pw}(T) \ \frac{\partial T(X,t)}{\partial t} \tag{4-7}$$

is needed throughout the thickness of the wall. In this equation k_w represents the thermal conductivity of the wall material, ρ_w is its density, and c_{pw} is its specific heat. A very good approximate solution can be obtained by using a finite-difference numerical technique. This technique can be viewed as a process in which 1) the solid is divided into a group of slabs or layers (figure 4-2) and 2) an energy balance approximating equation 4-7 is written for each layer in terms of finite temperature, time, and coordinate differences. The energy equations can be rearranged to express the current slab temperatures, $T(t + \Delta t)$, in terms of the previous temperatures, $T(t)$, and the previous surface fluxes, $\dot{q}_w''(t)$ and $\dot{q}_{wo}''(t)$. The resulting equations are

$$T_1(t + \Delta t) = T_1(t) \ (1 - a_1\Delta t) + a_1\Delta t \ T_2(t) + \frac{\Delta X}{k_w} \ \dot{q}_w''(t + \Delta t) \tag{4-8}$$

$$T_j(t + \Delta t) = T_j(t) \ (1 - a_j\Delta t) + a_j\Delta t \ \left[T_{j-1}(t) + T_{j+1}(t)\right] \tag{4-9}$$

$$T_N(t + \Delta t) = T_N(t) \ (1 - a_N\Delta t) + a_N\Delta t \ T_{N-1}(t)$$

$$- \frac{\Delta X}{k_{wN}} \ \dot{q}_{wo}''(t + \Delta t) \tag{4-10}$$

11

where $\quad a_j = \dfrac{2k_{wj}}{\rho c_{pwj}\Delta X^2}$ $\qquad$ (4-11)

$k_{wj} = k_w(T_j)$

$c_{pwj} = c_{pw}(T_j)$

$\Delta t \leq$ minimum of $1/a_j$

$N \leq 20$

$T_1 = T_{wu}$ or T_{wl} are upper wall slab temperatures when $T_1 = T_{wu}$

T_2 to T_N are lower wall slab temperatures when $T_1 = T_{wl}$

The energy balance at the upper layer gas-wall interface can then be expressed as

$$f_5 = \dot{q}''_{ku}(t + \Delta t) - \dot{q}''_{ru}(t + \Delta t) - \dot{q}''_{cu}(t + \Delta t) = 0 \qquad (4-12)$$

where

$$\dot{q}''_{ku} = \frac{1}{2}\,\rho_w\,c_{pw}(T_{wu})\Delta X\;\frac{T_{wu}(t + \Delta t) - T_{wu}(t)}{\Delta t}$$

$$\qquad (4-13)$$

$$+\;\frac{k_{wu}(T_{wu})}{\Delta X}\left[T_{wu}(t) - T_2(t)\right]$$

$\dot{q}''_{r\mu}$ $\quad$ is the net flux radiated to the inner (exposed) surface of the upper wall,

$\dot{q}''_{cu}$ $\quad$ is the flux convected to the inner wall surface, and

T_2 $\quad$ is obtained from equation 4-9.

Similarly, the energy balance at the lower gas-wall interface can be expressed as

$$f_6 = \dot{q}''_{k1}(t + \Delta t) - \dot{q}''_{r1}(t + \Delta t) - \dot{q}''_{c1}(t + \Delta t) = 0 \qquad (4\text{-}14)$$

where

$$\dot{q}''_{k1} = \frac{1}{2} \rho_w \, c_{pw}(T_{w1}) \Delta X \, \frac{T_{w1}(t + \Delta t) - T_{w1}(t)}{\Delta t}$$

$$(4\text{-}15)$$

$$+ \frac{k_{w1}(T_{w1})}{\Delta X} \left[T_{w1}(t) - T_2(t) \right]$$

$\dot{q}''_{r1}$ is the net flux radiated to the lower inner wall surface,

$\dot{q}''_{c1}$ is the flux convected to the lower inner wall surface, and

T_2 is obtained from equation 4-9.

5.   TRANSIENT MODEL FOR CRIBS BURNING IN AN ENCLOSURE

The conservation equations presented in section 4 must be augmented with a transient sub-model for pyrolyzing cribs in order to complete a transient model for cribs burning in an enclosure. The following pyrolysis model relates the time-dependent fuel pyrolysis rate, $\dot{m}_v$, to the free-burn pyrolysis rate, $\dot{m}''_{vo}$; the effective heat of vaporization, L_{vap}; the oxygen concentration in the lower layer, Y_{ox1}; and the radiant flux incident upon the cribs, $\dot{q}''_{rc}$.

$$f_7 = \dot{m}_v(t + \Delta t) - \dot{m}''_{vo}(t + \Delta t) \, A_i(Y_{ox1}(t + \Delta t)/0.23)$$

$$(5\text{-}1)$$

$$- (\dot{q}''_{rc}(t + \Delta t) \, A_c/L_{vap}) = 0$$

In this expression A_i and A_c are the internal and external surface areas of the crib, respectively. Details of the calculation of these areas and $\dot{q}''_{rc}$ are presented in reference [12].

In summary, the basic equations of the transient model for crib fires in an enclosure are

a. Mass balance for the enclosure:
    (equation 4-3)

b. Mass balance for the lower layer:
    (equation 4-4)

c. Energy balance for upper layer:
    (equation 4-5)

d. Energy balance for lower layer:
    (equation 4-6)

e. Energy balance at the upper gas-wall interface:
    (equation 4-12)

f. Energy balance at the lower gas-wall interface:
    (equation 4-14)

g. Fuel pyrolysis rate
    (equation 5-1)

6. RESULTS OF CALCULATIONS FOR WOOD CRIBS BURNING IN AN ENCLOSURE

The following calculation simulates the burning of four closely spaced
wood cribs located near the center of the room shown in figure 6-1. The room
surfaces are calcium silicate board. The experimental time-dependent free-
burn (no enclosure) mass loss rate of the four cribs, $\dot{m}_{vo} = \dot{m}''_{vo}(t) A_i$, is
shown in figure 6-2. For the calculation, the actual mass loss rate was
approximated by the two linear segments shown in the figure. Unless otherwise
specified, the remaining thermophysical properties and model parameters used
in the calculation are the same used in reference [12].

Initially, the effect of the gas layer transient terms was evaluated.
Two calculations were made; one with and another without the time derivative
terms in equations 4-3 to 4-6. Transient wall effects (equations 4-13 and
4-15) were included in both calculations. The heat of combustion, ΔH, was set
at 15,000 kJ/kg and the effective heat of vaporization, L_{vap}, was fixed at
1900 kJ/kg. Results depicting the first 150 seconds of simulated time are
presented in figure 6-3. The effect of the gas layer transients is shown to
be small after approximately 60 seconds.

14

The calculation which retained the gas layer transient terms was repeated using a slightly lower heat of combustion, ΔH = 13,000 kJ/kg. Figures 6-4 to 6-6 compare these results with experimental results for the same configuration. Two of the solid-line plots in figure 6-4 are identified as experimental upper wall and ceiling temperatures. The remaining solid lines in this figure represent experimental floor-to-ceiling gas temperatures measured at equally spaced locations along a vertical line. These solid lines tend to cluster in the upper and lower regions of the figure, thereby indicating the two-layer nature of the gas widely-spaced traces between these clusters correspond to the transition region between layers. The comparisons in figures 6-4 to 6-6 demonstrate the ability of the transient model to predict the major features of the experimental results.

7. DEVELOPMENT OF AN ENCLOSURE CORNER WALL FIRE MODEL

The transient model for a crib or cribs burning in an enclosure was treated as a uniform fixed-area fire which changed in intensity depending on its free-burn behavior, the incident radiant flux, and the available oxygen. The corner wall fire situation is more complicated because 1) the burning or pyrolyzing occurs over an extended area which is subject to non-uniform radiation and oxygen exposures and 2) the boundary of the involved area changes locally with time, because of the non-uniform exposure conditions.

In the following sections a wall fire spread zone model will be developed which features local pyrolysis rates and flame spread rates as functions of incident radiation and "local" oxygen concentration. In the context of the two-layer zone model, "local" oxygen concentration is the concentration in the gas layer (either the upper or lower layer) adjacent to the pyrolyzing surface.

7.1 Burning and Flame Spread Rates

Tewarson [1,2] and others have experimentally shown that, for relatively small horizontal upward-facing specimens under non-flaming and generally steady conditions, the mass loss or pyrolysis rate, $\dot{m}_v$, is a linear function of applied radiant heat flux, $\dot{q}_i''$. They have also shown that under flaming or

15

burning conditions $\dot{m}_v$ is both a linear function of $\dot{q}_i''$ and local oxygen concentration, Y_{ox}. Such functional dependencies will be assumed in this analysis for wall fire spread. Thus, for non-flaming conditions $\dot{m}_v$ per unit area will be expressed as [1,2,15]

$$\dot{m}_v'' = \begin{cases} 0; & \dot{q}_i'' \leq \dot{q}_i''^{**} \\ (\dot{q}_i'' - \dot{q}_i''^{**})/L_{vap}; & \dot{q}_i'' \geq \dot{q}_i''^{**} \end{cases} \tag{7-1}$$

where L_{vap} is the effective heat of vaporization and $\dot{q}_i''^{**}$ is the minimum heat flux to cause mass loss. Similarly, under flaming conditions $\dot{m}_v''$ will be taken as

$$\dot{m}_v'' = \dot{m}_v''^* + \xi(Y_{ox} - Y_{ox}^*) + (\dot{q}_i'' - \dot{q}_i''^*)/L_{vap} \tag{7-2}$$

where ξ is a constant and the "starred" terms depend on the reference state. For the example to be considered, the reference state will be at normal air conditions so $\dot{m}_v''^*$ represents the burn rate in air, $Y_{ox}^* = 0.233$, and $\dot{q}_i''^*$ is the minimum heat flux to sustain burning. Over a range of oxygen and flux levels, it has been found [1,2] that a critical fuel supply rate is needed to sustain burning; i.e.,

$$\dot{m}_v''(Y_{ox}, \dot{q}_i'') \geq \dot{m}_{v,crit}'' \tag{7-3}$$

For a number of materials this burning limit appears to be approximately 5 g/m-s. Also it is obvious that burning will not be possible at $Y_{ox} = 0$ (or a small, but finite value) regardless of the heat flux. Hence, the specific mass loss rate is given by Eq. (7-2) as long as Eq. (7-3) holds and Y_{ox} is in excess of some specified critical value, $Y_{ox,crit}$. Otherwise $\dot{m}_v''$ is given by Eq. (7-1). Consequently, the overall mass loss rate is given by

$$\dot{m}_v = \iint_{A_{inv}} \dot{m}_v'' \, dA \tag{7-4}$$

where A_{inv} is the involved area (burning plus pyrolyzing). The overall burning rate is

$$\dot{m}_b = \text{smaller of} \begin{cases} \iint_{A_b} \dot{m}_v'' \, dA \\ \text{or} \\ \dot{m}_a / r \ \text{(ventilation limit)} \end{cases} \tag{7-5}$$

where A_b is the burning area, $\dot{m}_a$ is the air flow rate through the doorway, and r is the stoichiometric air-to-fuel mass ratio.

Quintiere [1] has also shown that the results obtained from a radiant panel lateral flame spread apparatus can be expressed in the form

$$v_f = \left[C(\dot{q}_{i,ig}'' - \dot{q}_i'') \right]^{-2} \tag{7-6}$$

where v_f is the maximum flame spread rate for an incident flux $\dot{q}_i''$ which is not "too close" to the minimum flux for piloted ignition, $\dot{q}_{i,ig}''$, and C is an empirical material constant.

Both theoretical and experimental work [3-6] show flame spread rate to vary as Y_{ox}^m, where m is in range 0.9 to 3.6, depending upon the material, its thickness, and the value of Y_{ox} relative to $Y_{ox,crit}$. Incorporating this oxygen dependence into Eq. (7-6) yields

$$v_f = \frac{(Y_{ox}/0.233)^m}{\left[C(\dot{q}_{i,ig}'' - \dot{q}_i'') \right]^2} \tag{7-7}$$

For $\dot{q}_i''$ approaching and exceeding $\dot{q}_{i,ig}''$, modification to Eq. (7) is necessary. As a first approximation an upper bound, v_∞, is specified for v_f. There is also a lower flux limit, $\dot{q}_i''^*$, below which no opposed-flow flame spread occurs. Therefore,

$$v_f = \begin{cases} 0; \ \text{when} \ \dot{q}_i'' < \dot{q}_i''^* \\ \text{smaller of} \ v_\infty \ \text{and Eq. (7-7); when} \ \dot{q}_i''^* \leq \dot{q}_i'' < \dot{q}_{i,ig}'' \\ v_\infty, \ \text{when} \ \dot{q}_i'' \geq \dot{q}_{i,ig}'' \end{cases} \tag{7-8}$$

In this formulation the spread will cease when Y_{ox} is zero, although, in reality, the pyrolysis front would continue to advance if the incident flux

17

were sufficient. In the implementation of the wall flame spread examples only lateral opposed flow flame spread will be considered up to the time when Y_{ox} in the adjacent layer becomes zero. It is recognized that flame spread in the ceiling jet and downward spread are also present and will have to be included in a more complete analysis.

7.2 Wall Grid

Since the radiation incident upon a wall area element and the oxygen concentration to which it is exposed are position dependent, it is necessary to establish a grid for locating the involved wall elements. The grid for tracking the area of involvement on one wall is shown in figure 7-1. The grid for the adjacent wall is merely the mirror image of the first with respect to the left hand boundary (room corner). Each wall is represented by k equal-height horizontal strips. Initially, burning is assumed to exist on both walls from floor to ceiling over a horizontal distance, δ_i, measured from the corner. Subsequent flame spread is restricted to the horizontal direction. At the end of each time step, Δt, new flame-front positions are established for each horizontal strip. Differences between flame-front positions at the beginning and end of each time step establish the added area of involvement.

The center coordinates of each area element are used to compute the local radiant flux and oxygen concentration which are then used to compute $\dot{m}_v''$ or $\dot{m}_b''$ for the element. The coordinates at the centers of leading edges of the newest elements are used to compute the flame spread rates at these edges. These coordinates are included in figure 7-1.

7.3 Local Radiant Flux to Wall

Incident radiant flux is needed as a function of position on the wall to evaluate the local pyrolysis rates and flame spread rates of the developing wall fire. This flux is made up of contributions from the hot upper gas layer, the hot wall surfaces in both layers, and the flames on the involved portions of the walls. Details of the flux calculations are presented in the following sections.

18

7.3.1 Radiation from Enclosure Surfaces and Upper Gas Layer

For this calculation, all enclosure surfaces are assumed to be non-burning and at a temperature T_{wu} or T_{wl} (figure 7-2). Radiation from these surfaces and the upper gas layer to any point on a wall is computed using standard geometrical exchange factors [16] and the mean-beam-length approximation [17,18].

Consider a target wall element located within the lower gas layer (figure 7-3). The element receives radiation from the four quadrants designated $i = 1$ to 4. Sub-regions $i = 5$ in the third quadrant and $i = 6$ in the fourth quadrant identify the portions of these quadrants which lie in the upper layer. The parameter $F_{dA,i}$ is the geometrical factor between the target element dA and the enclosure surfaces which bound the ith volume.

The effective emissivity of the upper-layer gas within a quadrant is obtained from the mean-beam-length approximation

$$\varepsilon_{g,i} = 1 - e^{-k_g L_{m,i}} \qquad (7-9)$$

where the mean beam length

$$L_{m,i} = 4 \times \frac{\left[\begin{array}{l}\text{volume of upper layer in}\\ \text{quadrant containing ith region}\end{array}\right]}{\left[\begin{array}{l}\text{surface area of upper-layer}\\ \text{volume in quadrant containing}\\ \text{ith region.}\end{array}\right]} \qquad (7-10)$$

If the emissivities of the solid surfaces are assumed to be unity, then it can be shown (Appendix B) that the radiation from the upper gas layer and enclosure surfaces to a target element located in the lower layer can be expressed as

$$\dot{q}''_{gw} = \sum_{i=1}^{4} \sigma F_{dA,i} T_{wl}^4 + \sum_{i=5}^{6} \sigma F_{dA,i} \left[\varepsilon_{g,i} T_{gu}^4 + (1 - \varepsilon_{g,i}) T_{wu}^4 - T_{wl}^4\right] \qquad (7-11)$$

When the element is located in the upper layer the expression becomes

19

$$\dot{q}''_{gw} = \sum_{i=1}^{4} \sigma F_{dA,i} \left[\epsilon_{g,i} T_{gu}^4 + (1 - \epsilon_{g,i}) T_{wu}^4 \right]$$

$$+ \sum_{i=5}^{6} \sigma F_{dA,i} (1 - \epsilon_{g,i}) (T_{wl}^4 - T_{wu}^4)$$

(7-12)

where the geometrical factors apply to the inverted forms of the geometries shown in figure 7-3; i.e., quadrants $i = 1$ and 2 contain portions of the upper layer and $i = 3$ and 4 contain portions of the upper and lower layers.

7.3.2 Radiation from Burning Wall Area

7.3.2.1 Radiation from Burning Wall to Adjacent Burning Wall

Each burning area element contributes to the radiant flux incident upon the adjacent burning wall (figure 7-4) according to the expression

$$d\dot{q}''_f = \dot{q}''_e F_{s,r} e^{-(k_g \ell_g)}$$

(7-13)

where $d\dot{q}''_f$ is the incident flux at the "receiver",

  k_g is the upper-layer attenuation coefficient,

  ℓ_g is the path length through the upper layer (Appendix C), and

  $F_{s,r}$ is the geometrical factor between the receiver at surface element r and source at surface element s.

The flux emitted from the source element, $\dot{q}''_e$, is expressed as

$$\dot{q}''_e = \sigma T_f^4 (1 - e^{-k_f \ell_f}) + \epsilon_s \sigma T_s^4 e^{-k_f \ell_f}$$

(7-14)

where the first term on the right represents flux from the flame and the second term accounts for flux from the wall surface behind the flame. The parameters k_f and ℓ_f are flame attenuation coefficient and flame thickness, respectively. It appears from equation 7-14 that $\dot{q}''_e$ will vary from material to material. However, since data of this type are scarce, $\dot{q}''_e$ was approximated

20

in the current calculations as a constant of 20 kW/m^2. This value falls
between the "thin" and "thick" flame values estimated by Modak and Orloff [19]
for vertical polyurethane surfaces. The total flux incident upon a burning
wall element from the burning areas, A_b', of an adjacent wall is obtained by
summing equation 7-13 over all burning elements;

$$\dot{q}_f'' = \sum_{A_b'} \dot{q}_e'' \, F_{s,r} \, e^{-k_g \ell_g} \tag{7-15}$$

7.3.2.2 Radiation from Flames on Burning Wall to Same Wall

It is assumed that radiation transferred from flames on a wall to a spot
on the same wall has been accounted for in the test-method-based analytical
expressions for burning and flame spread rates; that is, these fire properties
are independent of burning area.

7.3.3 Total Incident Radiation

For the purposes of computing pyrolysis and flame spread rates, the
radiant flux, $\dot{q}_i''$, to a point on a wall is

$$\dot{q}_i'' = \dot{q}_{gw}'' + \dot{q}_f'' - \sum_{A_b'} F_{s,r} \, \sigma \, T_{wj}^4 \tag{7-16}$$

where $\dot{q}_{gw}''$ is defined by either equation 7-11 or 7-12, $\dot{q}_f''$ is given by
equation 7-15, and the remaining term on the right compensates for the fact
that the wall area behind the burning region is included in both $\dot{q}_{gw}''$ and $\dot{q}_f''$.
The parameter T_{wj} is either T_{wu} or T_{wl}.

7.4 Wall Fire Entrainment

A complete theory for wall fire entrainment does not exist. Neverthe-
less, an approximate entrainment model will suffice for the present task.
Indeed, a simple point source buoyant plume model will be adequate in view of
the approximations made in previous sections of this report and the prelimi-
nary nature of this project.

The mass flux, $\dot{m}_p$, a distance Z_e above an isolated point buoyancy source of strength Q is given [20] by

$$\dot{m}_p = 0.0625 \quad Q \quad Z_e^5 \quad 1/3 \tag{7-17}$$

For the wall fire, Q will be set equal to the total heat release rate of the burning wall area located in the lower gas layer and the point source will be located at the floor. Since the mass flux to the upper layer is needed, Z_e will be equated to the gas-interface height, Z_d.

7.5 Summary of Wall Fire Model Equations

The basic equations for the corner wall fire spread model are gas layer equations 4-3 to 4-6, wall equations 4-12 to 4-15, fire plume entrainment equation 7-17, and pyrolysis equation

$$f_7 = \dot{m}_v - \dot{m}_b - \sum_{A_{py}} \dot{m}_v'' v_f \, \Delta t \, \Delta Z = 0 \tag{7-18}$$

where

$$\dot{m}_v'' = \begin{cases} 0; \ \dot{q}_i'' \leq \dot{q}_i''^{**} \\ \\ (\dot{q}_i'' - \dot{q}_i''^{**})/L_{vap}; \ \dot{q}_i'' \geq \dot{q}_i''^{**} \end{cases} \tag{7-19}$$

$$\dot{m}_b = \sum_{A_b} \dot{m}_b'' v_f \, \Delta t \, \Delta Z \tag{7-20}$$

$$v_f = \begin{cases} 0; \ \dot{q}_i'' < \dot{q}_i''^{*} \\ \text{smaller of } v_\infty \text{ and equation 7-7; } \dot{q}_i''^{*} \leq \dot{q}_i'' < \dot{q}_{i,ig}'' \\ v_\infty; \ \dot{q}_i'' \geq \dot{q}_{i,ig}'' \end{cases} \tag{7-21}$$

$$\dot{m}_b'' = \dot{m}_b''^{*} + \xi(Y_{ox} - Y_{ox}^{*}) + (\dot{q}_i'' - \dot{q}_i''^{*})/L_{vap} \tag{7-22}$$

subject to the constraints

$$\dot{m}_b'' \geq \dot{m}_{b,crit}'' \tag{7-23}$$

22

$$Y_{ox} \geq Y_{ox,crit} \tag{7-24}$$

$$\dot{m}_b \leq \dot{m}_i/r \tag{7-25}$$

where Y_{ox} is either Y_{oxu} or Y_{oxl}, and

$\dot{q}_i''$ is given by equation 7-16.

Subsidiary equations A-1, A-2, A-4 to A-13, and A-16 to A-19 listed in Appendix A complete the model.

8. RESULTS OF WALL FIRE SPREAD CALCULATIONS FOR A HYPOTHETICAL WALL MATERIAL

The wall material is termed hypothetical because it was arbitrarily assigned artificial flame spread, burning rate, and stoichiometric properties which represent the properties of wood, polymethyl methacrylate (PMMA), or calcium silicate board. The values used in the calculation are presented in table 8-1. This arbitrary choice of properties was convenient and consistent with the limited objective of demonstrating the qualitative features of the model.

The allotted simulated time span for each calculation was 0 to 590 seconds. The time increment, Δt, was initially set at 10 seconds. In the event that mathematical convergence was not achieved at a given simulated time, Δt was halved, conditions from the previous time reinstated, and the calculation repeated. If this process reduced Δt to less than 0.3125 seconds, or if Y_{oxu} became equal to 0, the calculation was terminated. Finally, it should be noted that the last term in equation 7-16 -- the wall area correction term -- was not included in these calculations. Therefore, $\dot{q}_i''$ is exaggerated during the later portion of the simulation when T_{wu} becomes large.

The first configuration considered is shown in figure 7-5. At t = 0, uniform burning exists from floor to ceiling over a width δ_i = 0.5 m on each of two walls meeting at a corner. Calculated results at subsequent times are shown in figures 7-6 to 7-9. Since the area of involvement is symmetrical with respect to the room corner, only the pattern on one wall is shown. The

23

burning rates listed in these figures represent the totals for both walls. As previously stated, on account of the forementioned approximations and assumptions, results are intended to be viewed in a qualitative rather than a quantitative perspective.

Figure 7-6 shows the predicted conditions at t = 100 seconds. Only a small increase in area of involvement occurs up to this time because the incident radiant flux is still relatively low. Note that the spread is slightly less in the upper layer relative to that in the lower layer despite a higher incident flux in the former. The significantly lower oxygen concentration in the upper layer (Y_{oxu} = 0.135 versus Y_{oxl} = 0.209) more than offsets the higher radiation level, thereby producing less spread. Little change occurs in the area-of-involvement pattern until some time in excess of 200 seconds. The situation at t = 240 seconds is shown in figure 7-7. Spread in the upper layer begins to outdistance that in the lower layer because radiation has become the controlling factor. Within the next 5 seconds (figure 7-8) the spread increases rapidly in the upper layer as the incident radiation increases. Rapid growth occurs in both layers until t = 250 seconds (figure 7-9) when Y_{oxu} goes to zero and the calculation terminates.

The above results are summarized in figure 7-10. The properties of PMMA lead to a relatively low flame spread rate with a fire nearly fixed in area (A_{inv}) for an extended period. However, the high energy release rate per unit area of PMMA which was used in the calculation, and the subsequent feedback of a portion of this energy by the enclosure to the burning area produces a steadily increasing burning rate, $\dot{m}_b$, which appears to drive the system to an unstable or flashover condition.

The effect of the initial width of the burning area on each wall, δ_i, was then investigated. Figure 7-11 compares the upper layer gas temperature results, T_{gu}, for calculations of corner wall fires with δ_i equal to 0.50, 0.35, and 0.25 m. In each case, the initial burning area extended from floor to ceiling. Reducing δ_i from 0.50 to 0.35 m delays flashover by approximately 300 seconds, whereas the 0.25 m initial width fails to produce flashover within the simulated time span.

24

Figure 7-12 presents the results of a calculation representing a corner wall fire in a room with combustible lining on only the lower half of the walls. In this case, with $\delta_i = 0.5$ m, flashover does not occur within 590 seconds. Increasing δ_i to 0.8 m (figure 7-13) produces results only to 300 seconds, at which time mathematical convergence ceases. Nevertheless, the rates of increase of T_{gu}, $\dot{m}_b$, and $\dot{q}''_{il}$ just prior to 300 seconds suggest imminent flashover. Indeed, the failure to converge could be a consequence of rapid changes in the variables at the onset of flashover.

9. CONCLUSIONS

On the basis of the work carried out during this project the following conclusions are drawn.

a. A wall spread model has been produced which takes into account the oxygen and external flux dependencies of the flame spread and burning rate properties of lining materials. These dependencies in conjunction with a simple horizontal flame spread model were shown to produce aspects of the area-of-involvement pattern and flashover condition which are qualitatively reasonable. Many improvements are possible such as adding a ceiling-jet model and allowing for vertical as well as horizontal flame spread.

b. The constantly expanding wall-grid scheme used in the model was inefficient with respect to computation time. Alternative schemes, such as a predefined number of area elements which "turn on" as the fire spreads, should be explored.

c. A transient version of the quasi-steady enclosure fire model from reference [12] was a consequence of this project. Fair to good agreement between calculated and experimental results was demonstrated for a configuration of four wood cribs in a room. This model should be useful in future analyses of isolated fires within rooms.

d. Advancing the wall spread model from a qualitative to a quantitative tool will require experimental verification of the flame spread, burning rate, and entrainment sub-models for vertical surfaces. Efforts in these areas are underway at NBS.

10. ACKNOWLEDGMENTS

11. REFERENCES

[1] Tewarson, A. and Pion, R. F., Flammability of Plastics - I. Burning Intensity, Combustion and Flame, 26, 85-103 (1978).

[2] Tewarson, A., Experimental Evaluation of Flammability Parameters of Polymeric Materials, FMRC J.I., 1A6R1, Factory Mutual Research, Norwood, MA (February 1979).

[3] Magee, R. S. and McAlevy, III, The Mechanism of Flame Spread, J. Fire and Flammability, Vol. 2, 271-297 (October 1971).

[4] Fernandez-Pello, A. C. and Glassman, I., The Effect of Oxygen Concentration on Flame Spread in Opposed Forced Flow, 1979 Spring (Western States Section) Combustion Meeting, Brigham Young University, Salt Lake City, UT (April 23-24, 1979).

[5] Frey, A. E., Jr. and Tien, J. S., A. Theory of Flame Spread Over a Solid Fuel Including Finite Chemical Kinetics, Combustion and Flame, 36, 263-289 (1979).

[6] Maradey, J. F., Tien, J. S. and Prahl, J. M., The Upward and Downward Flame Propagation Limits of Rigid Polyurethane Foams, FTAS/TR-77-131, Case Western Reserve University, Cleveland, OH (September 1977).

[7] Quintiere, J. G., Growths of Fire in Building Compartments, Fire Standards and Safety, ASTM STP 614, American Society for Testing and Materials, Philadelphia, PA, 131-167 (1977).

[8] Emmons, H. W., Mitler, H. E. and Trefethen, L. N., Computer Fire Code III, Home Project Tech. Rept. No. 25, Harvard University, Cambridge, MA (1978).

[9] Pape, R. and Waterman, T., Modifications to the RFIRES Preflashover Room Fire Computer Model, IITRI Project J6400, IIT Research Institute, Chicago, IL (March 1977).

[10] MacArthur, C. D. and Meyer, J. F., Dayton Aircraft Cabin Fire Model Validation, Phase 1, Rept. No. FAA-RD-78-57, University of Dayton Research Institute, Dayton, OH (March 1978).

[11] Smith, E. E. and Heibel, J. T., Evaluating Performance of Cellular Plastics in Fire Systems, PRC Proj. No. RP-75-1-36, Ohio State University, Columbus, OH (1977).

[12] Quintiere, J. G. and McCaffrey, B. J., The Burning of Wood and Plastic Cribs in an Enclosure: Volume I, NBSIR 80-2054, National Bureau of Standards, Washington, D. C. (1980).

[13] Rockett, J. A., Modeling of NBS Mattress Tests with the Harvard Mark V Fire Simulation, NBSIR 81-2440, National Bureau of Standards, Washington, D. C. (1981).

[14] Tanaka, T., A Mathematical Model of a Compartment Fire, B.R.I. Report No. 70, Building Research Institute, Japan (February 1977).

[15] Quintiere, J. G., An Approach to Modeling Wall Fire Spread in a Room, Fire Safety Journal, Vol. 3, Nos. 2-4, 201-214 (January-March 1981).

[16] Sparrow, E. M. and Cess, R. D., Radiation Heat Transfer, Washington, D. C., Hemisphere Publishing Corp. (1978).

[17] Modak, A. T. and Matthews, M. K., Radiation Augmented Fires within Enclosures, Tech. Rept. 22361-8, Factory Mutual Research Corp., Norwood, MA (February 1977).

[18] Siegel, R. and Howell, J. R., Thermal Radiation Heat Transfer, Vol. III, NASA SP-164, National Aeronautics and Space Administration, Washington, D. C. (1971).

[19] Modak, A. T. and Orloff, L., Fires of Insulations on Tank Exteriors, Tech. Rept. J.I. OAOR9.BU RC79-BT-11, Factory Mutual Research Corp., Norwood, MA (October 1979).

[20] Zukoski, E. E., Kubota, T. and Centegen, B., Entrainment in Fire Plumes, Fire Safety Journal, Vol. 3, Nos. 2-4, 107-122 (January-March 1981).

[21] Tewarson, A., Physics-Chemical and Combustion/Pyrolysis Properties of Polymeric Material, NBS-GCR-80-295, National Bureau of Standards, Washington, D. C. (November 1980).

[22] Quintiere, J. G., A Simplified Theory for Generalizing Results from a Radiant Panel Rate of Flame Spread Apparatus, Fire and Materials, Vol. 5, No. 2 (1981).

WALL FIRE SPREAD FROM A CORNER
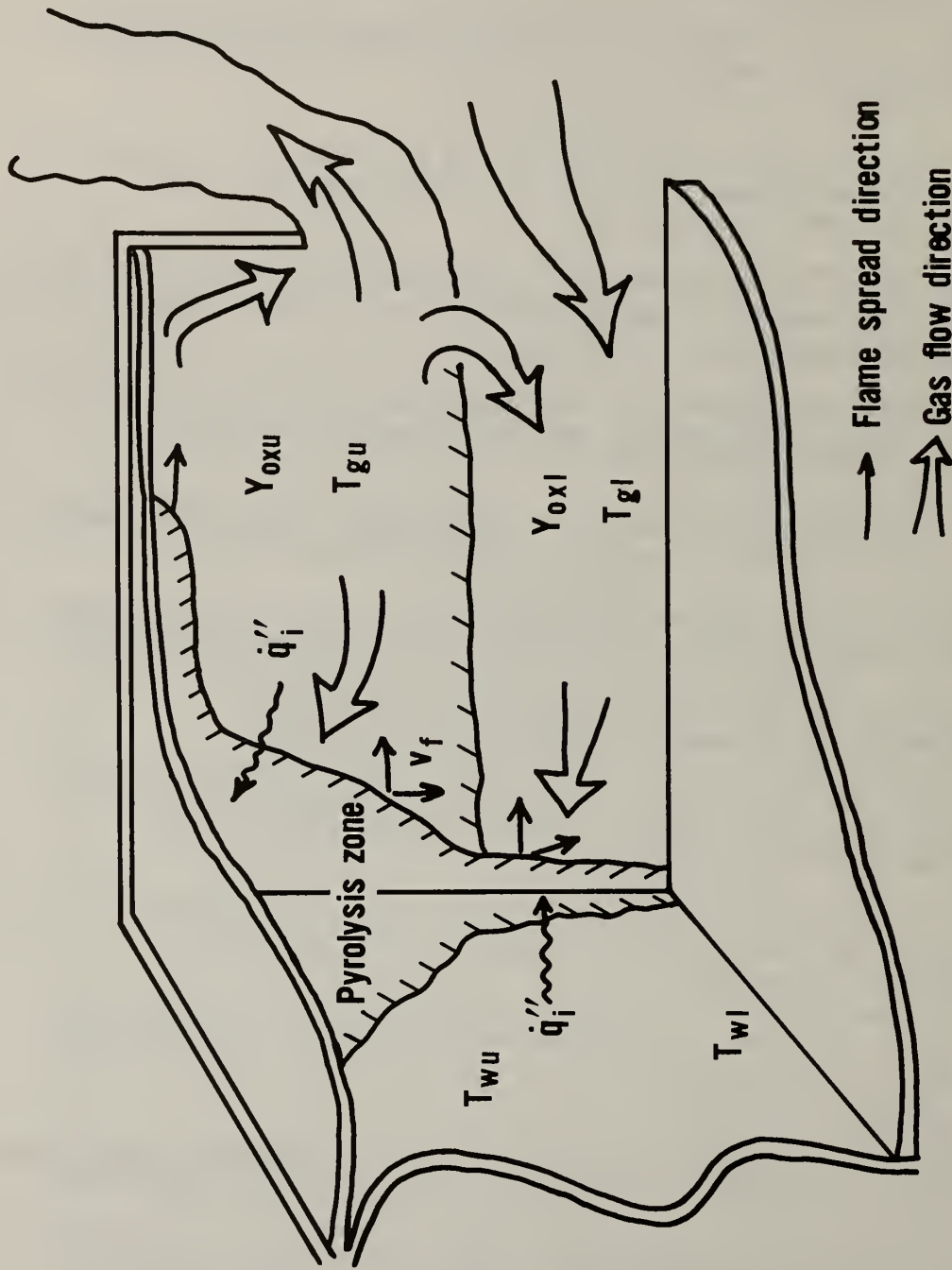
$v_f = v_f(Y_{ox}, \dot{q}_i'')$ - Flame spread rate

$\dot{m}_v'' = \dot{m}_v''(Y_{ox}, \dot{q}_i'')$ - Pyrolysis rate

Figure 1-1. All spread phenomena

APPROACH

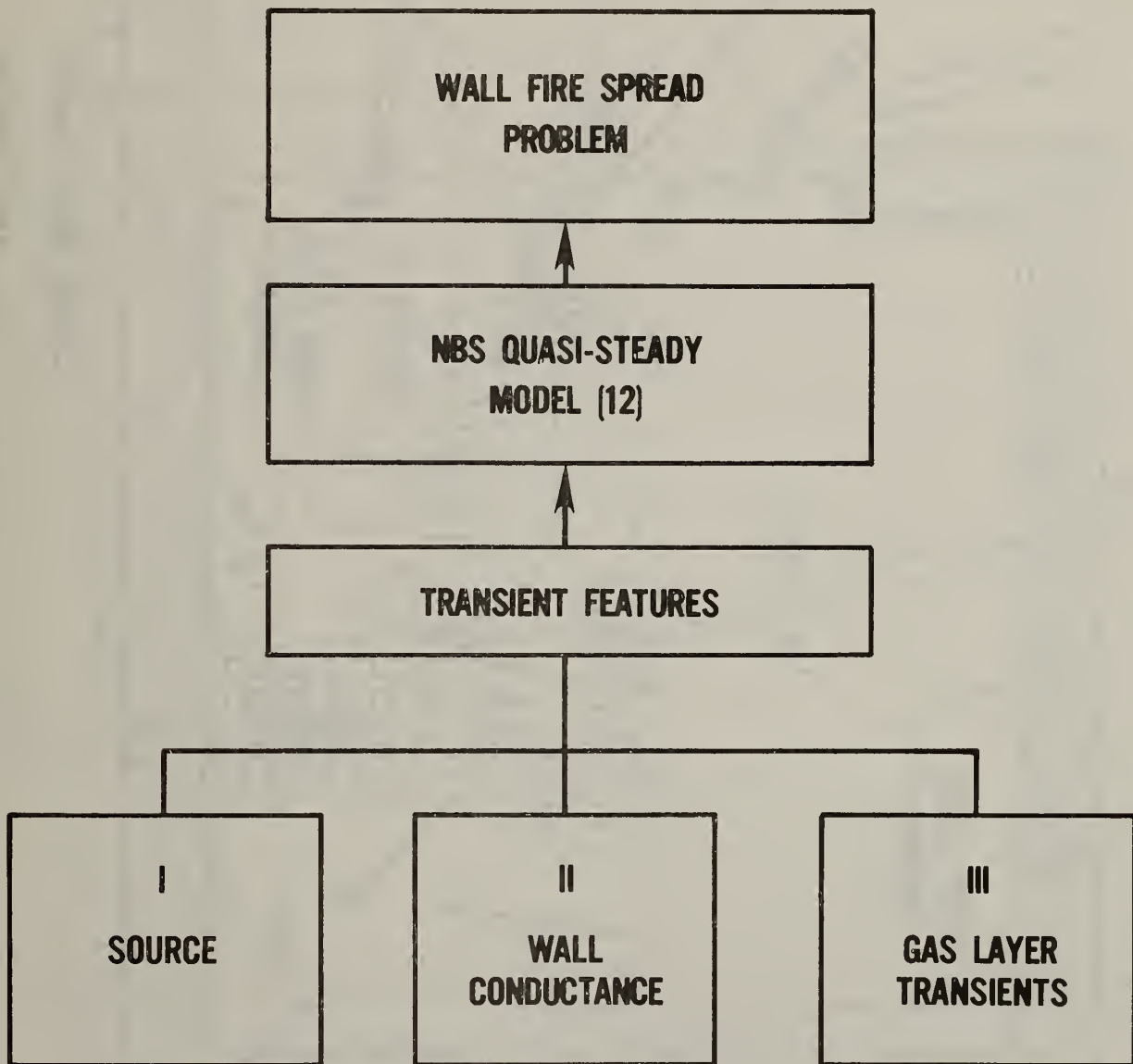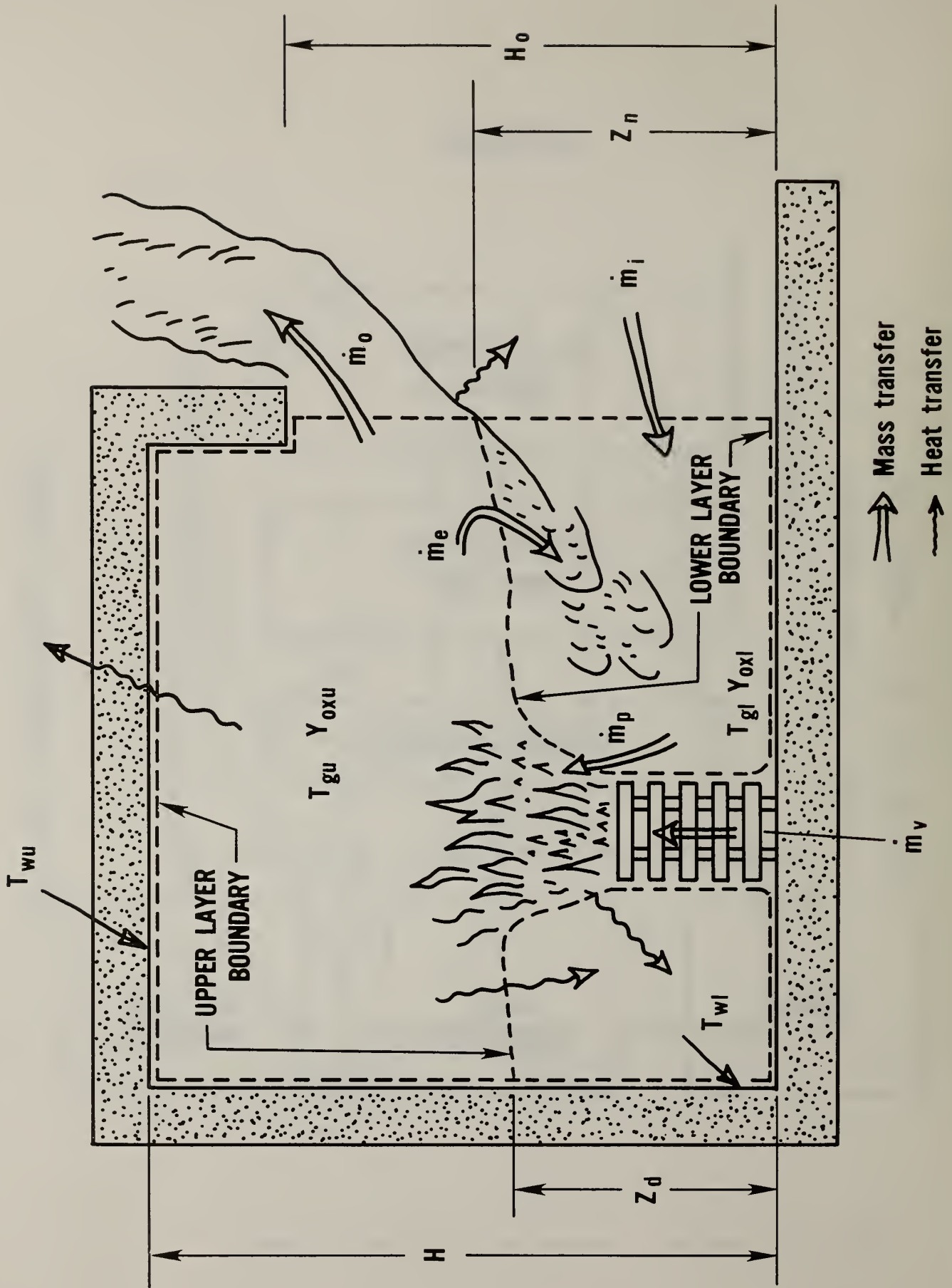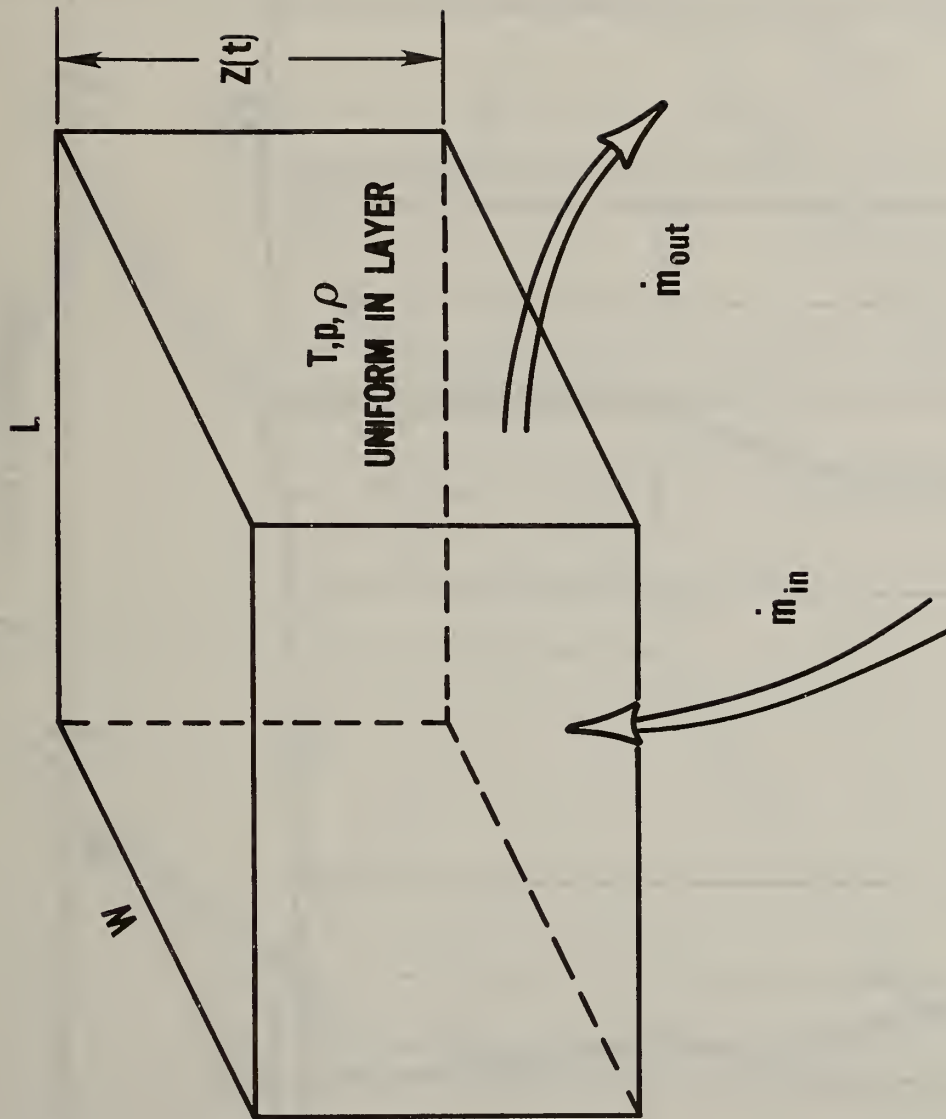Figure 2-1. Approach to solving wall fire spread problem

29

Figure 3-1. Two-layer zone model

$$\left[WL \frac{d}{dt} (\rho Z) + \dot{m}_{out} - \dot{m}_{in} = 0 \right]$$

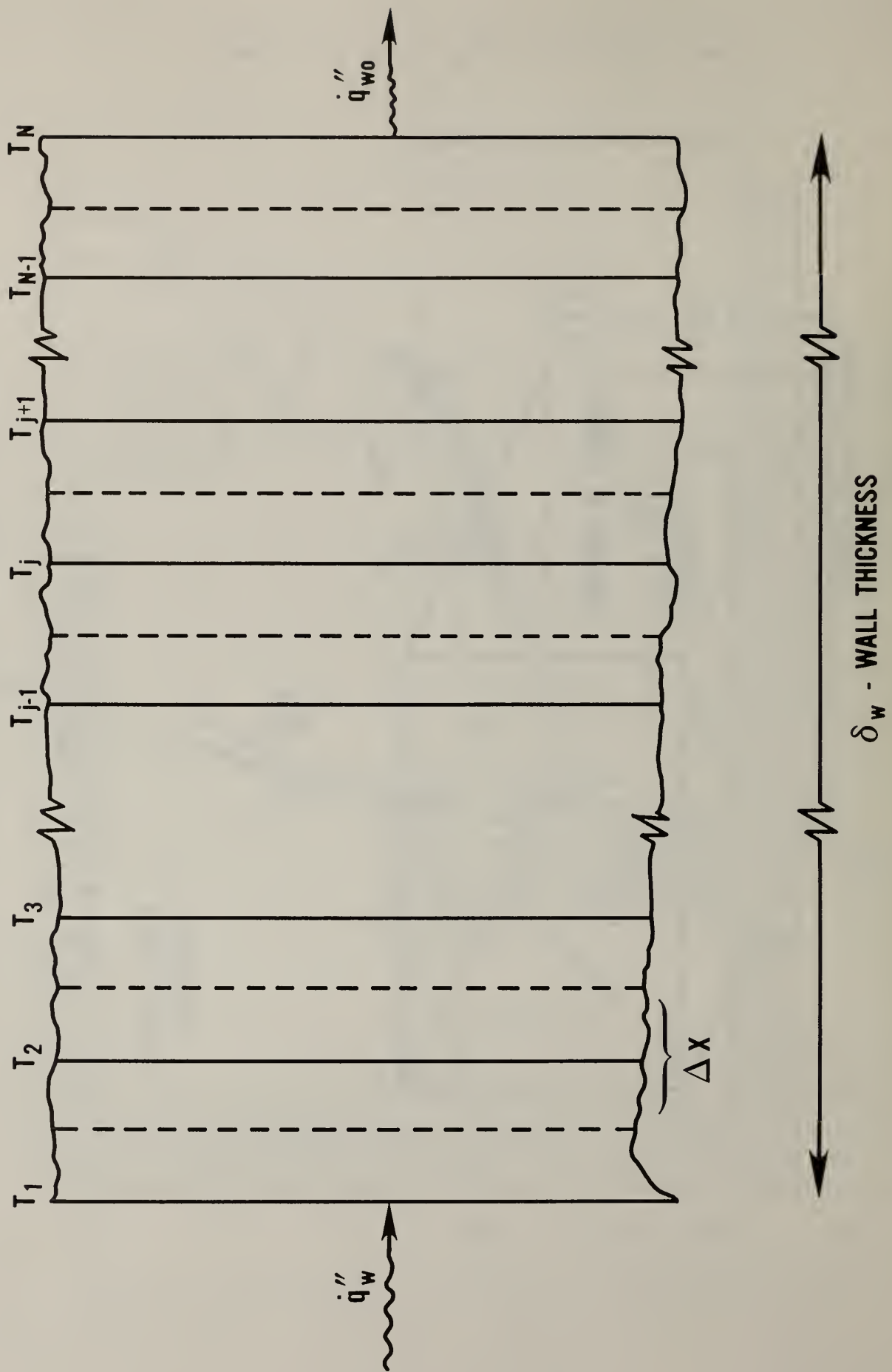Figure 4-1. Equation of continuity applied to g or layer
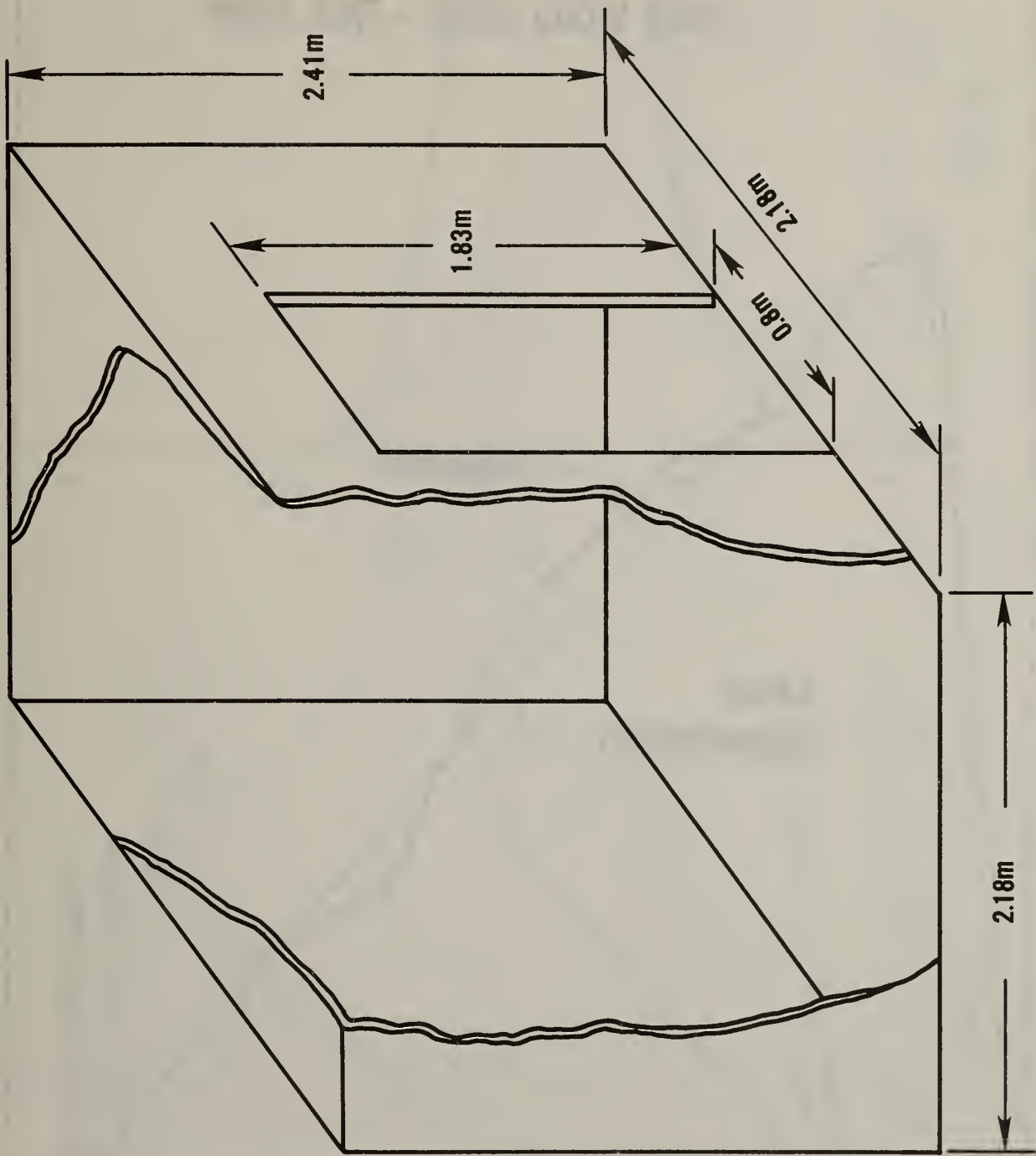
31

Figure 4-2. Finite-difference slabs

Figure 6-1. Room geometry used in calculations
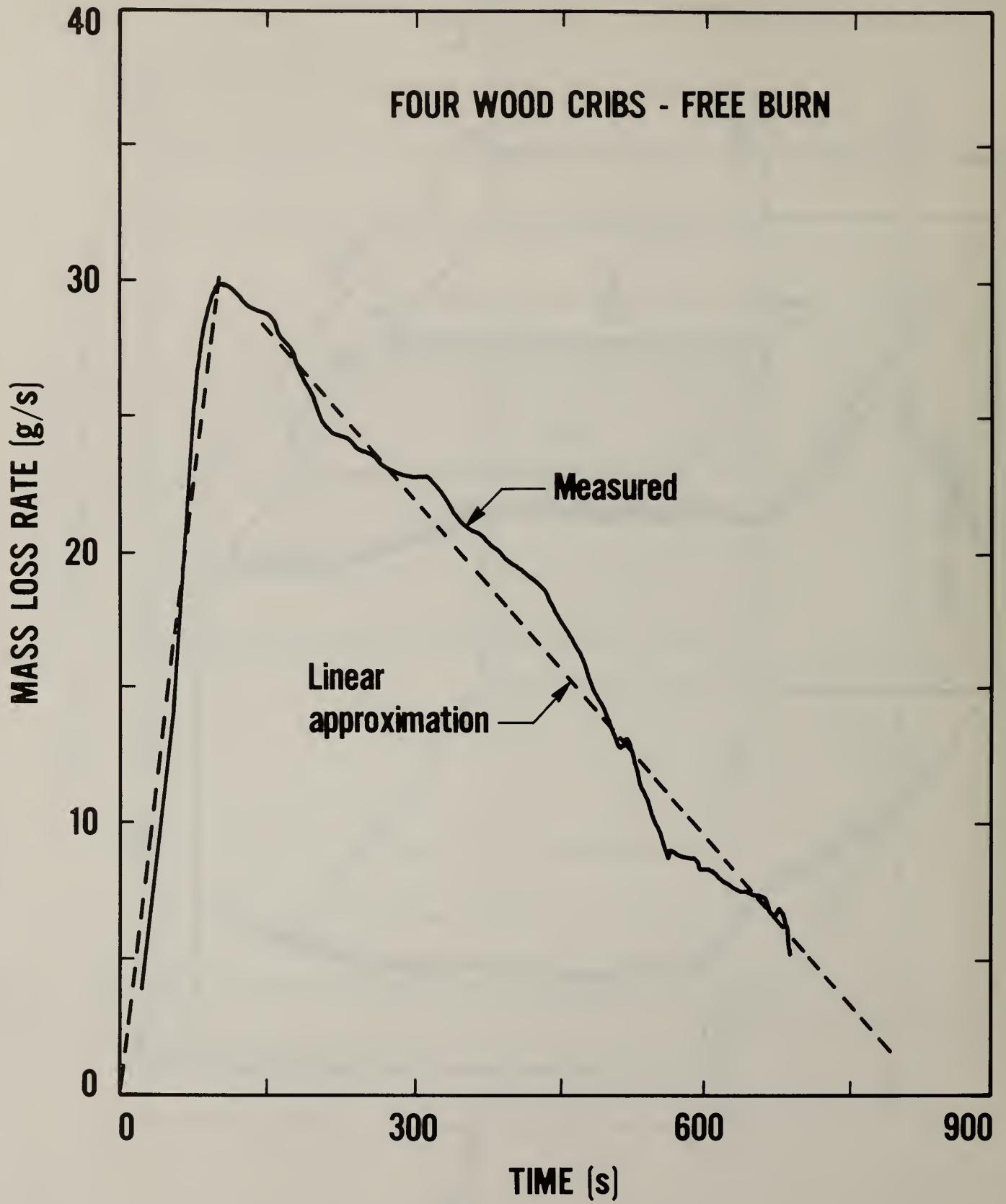
Figure 6-2. Fire-burn mass loss rate for four wood cribs
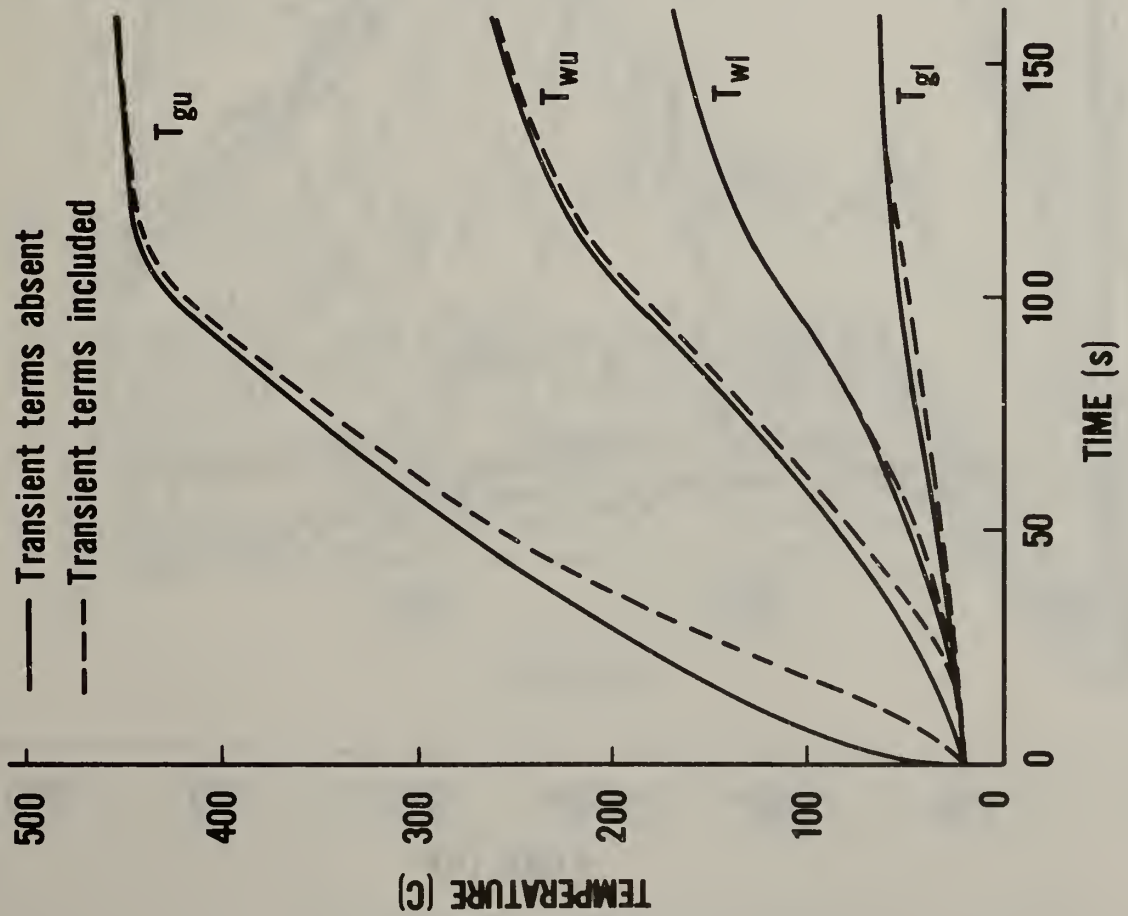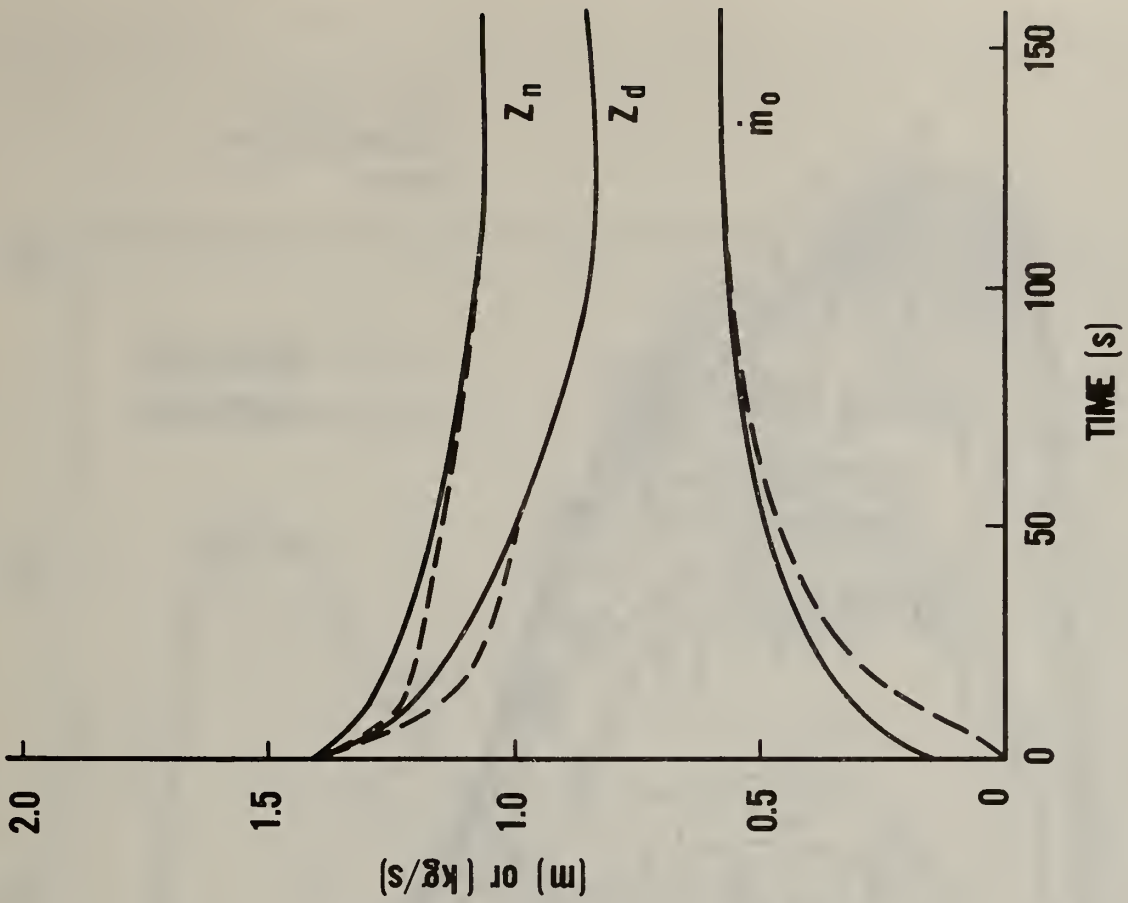
Figure 6-3. Effect of layer transient terms on wood-crib calculation
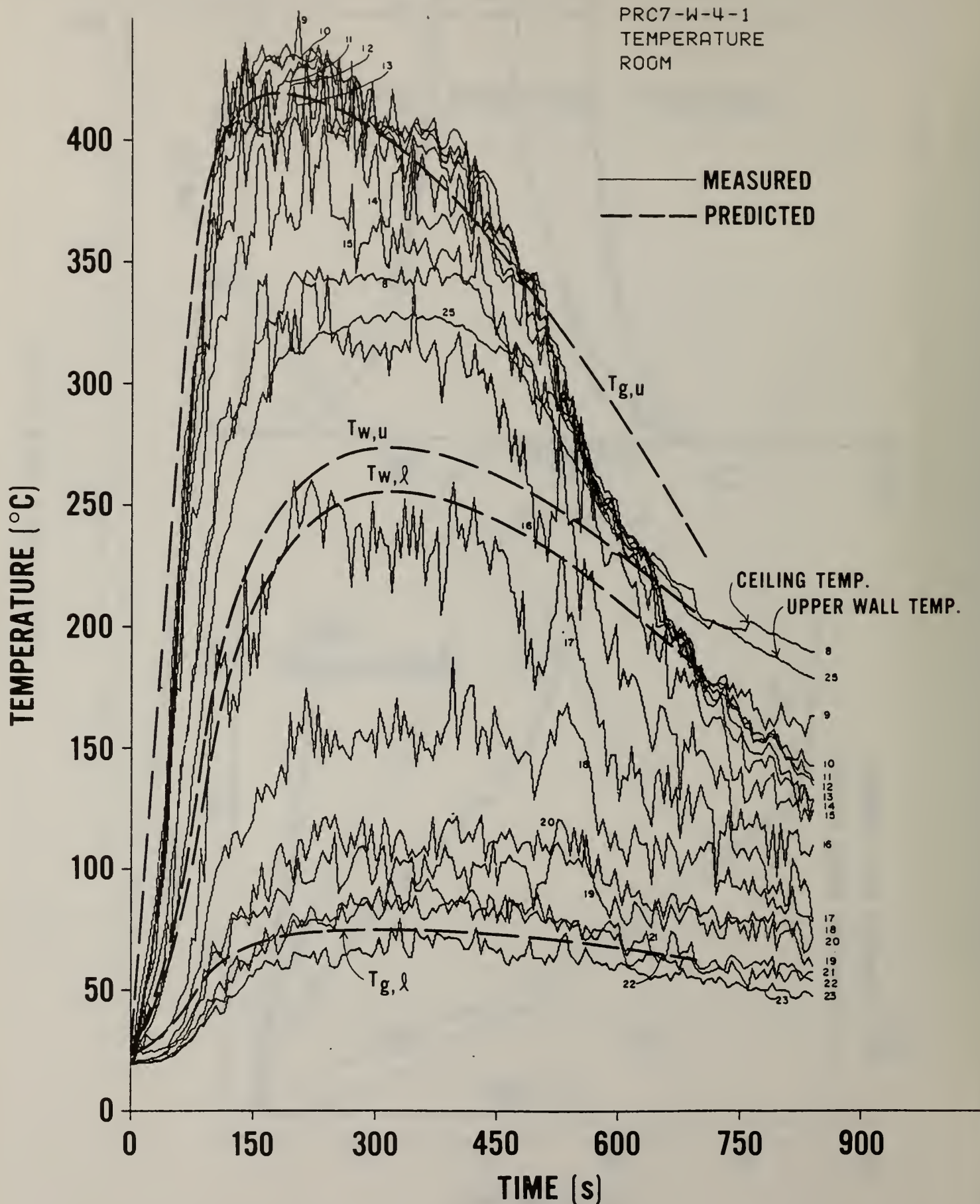
Figure 6-4. Comparison of experimental and theoretical enclosure
temperatures - - four wood cribs
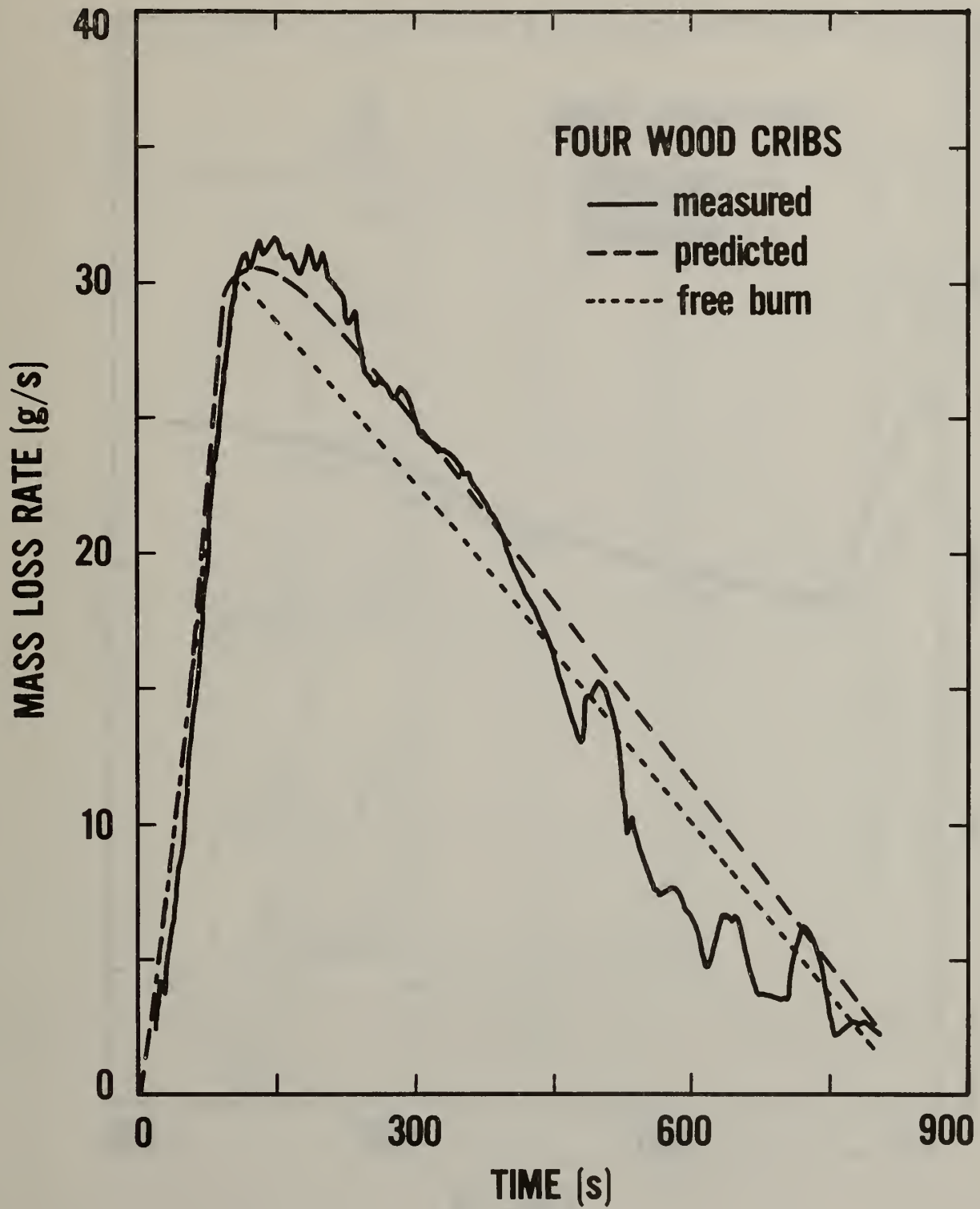
Figure 6-5. Comparison of experimental and theoretical mass loss
rate - - four wood cribs

37
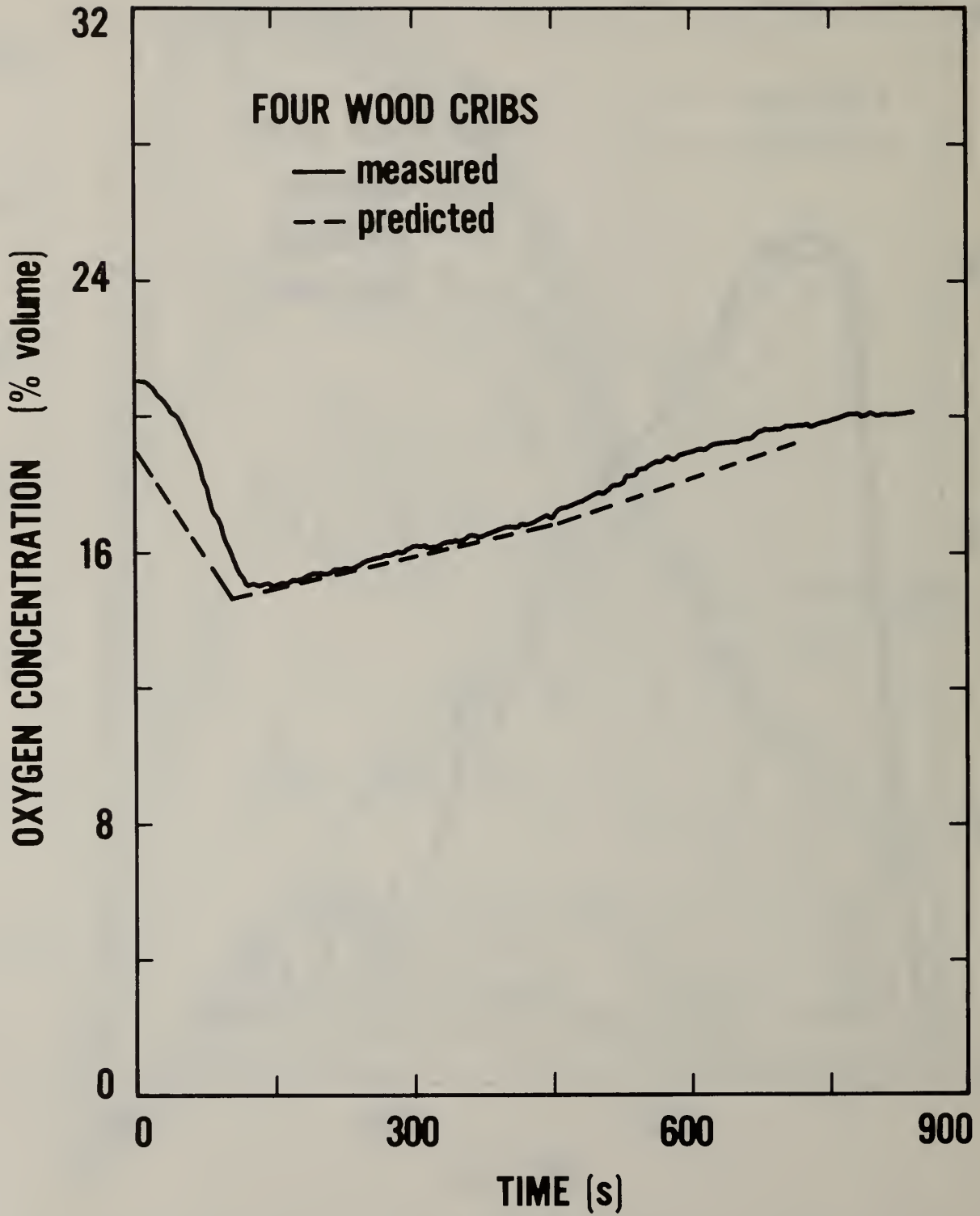
Figure 6-6.   Comparison of experimental and theoretical oxygen
concentrations - - four wood cribs

38

Figure 7-1. Grid for wall spread calculation
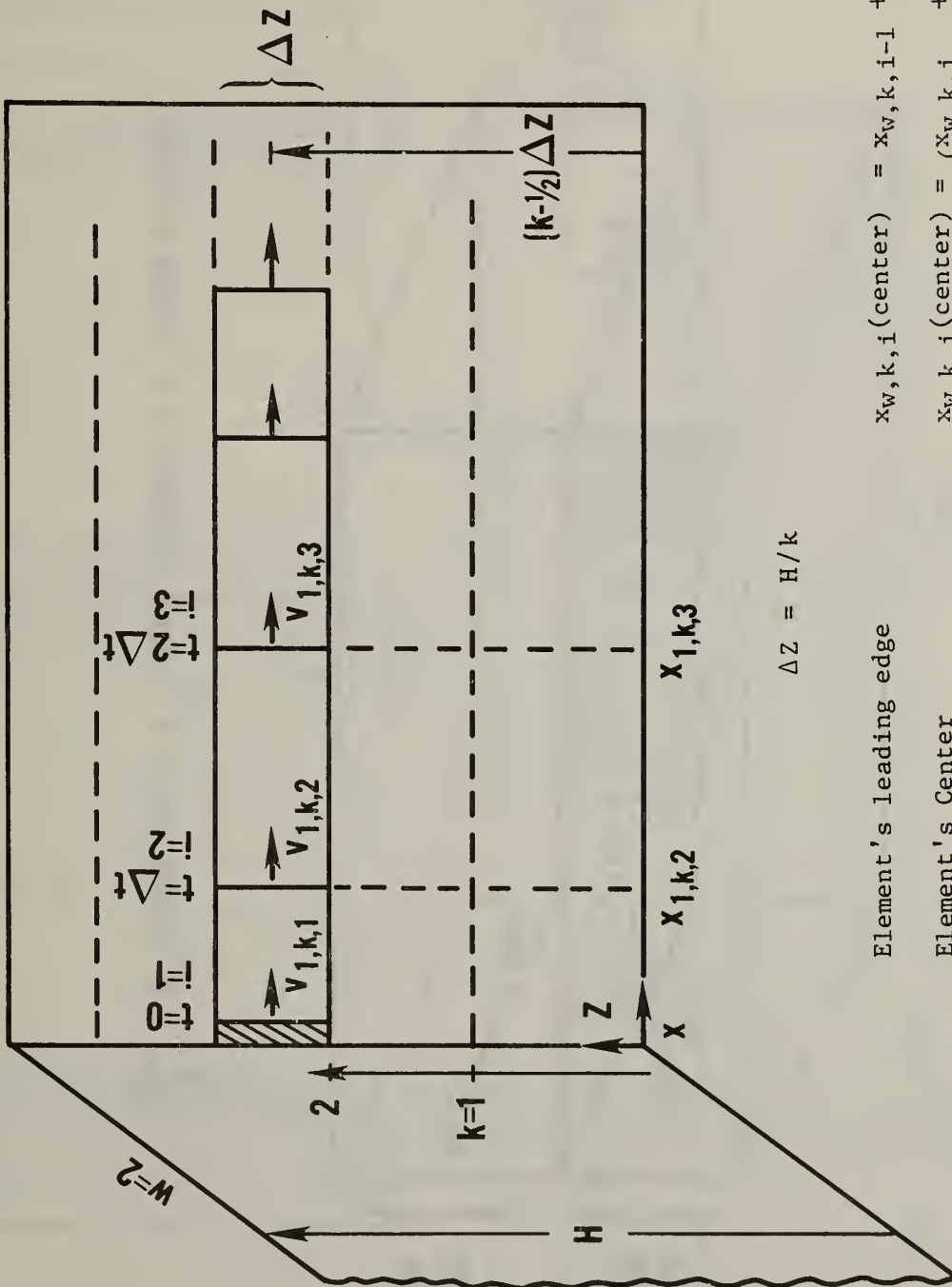
Element's leading edge $\quad x_{w,k,i}(\text{center}) = x_{w,k,i-1} + v_{w,k,i-1}\Delta t$

Element's Center $\quad x_{w,k,i}(\text{center}) = (x_{w,k,i} + x_{w,k,i-1})/2$

Element's horizontal centerline $\quad Z_{w,k,i}(\text{center}) = (k - 1/2)\Delta z$

$\Delta Z = H/k$
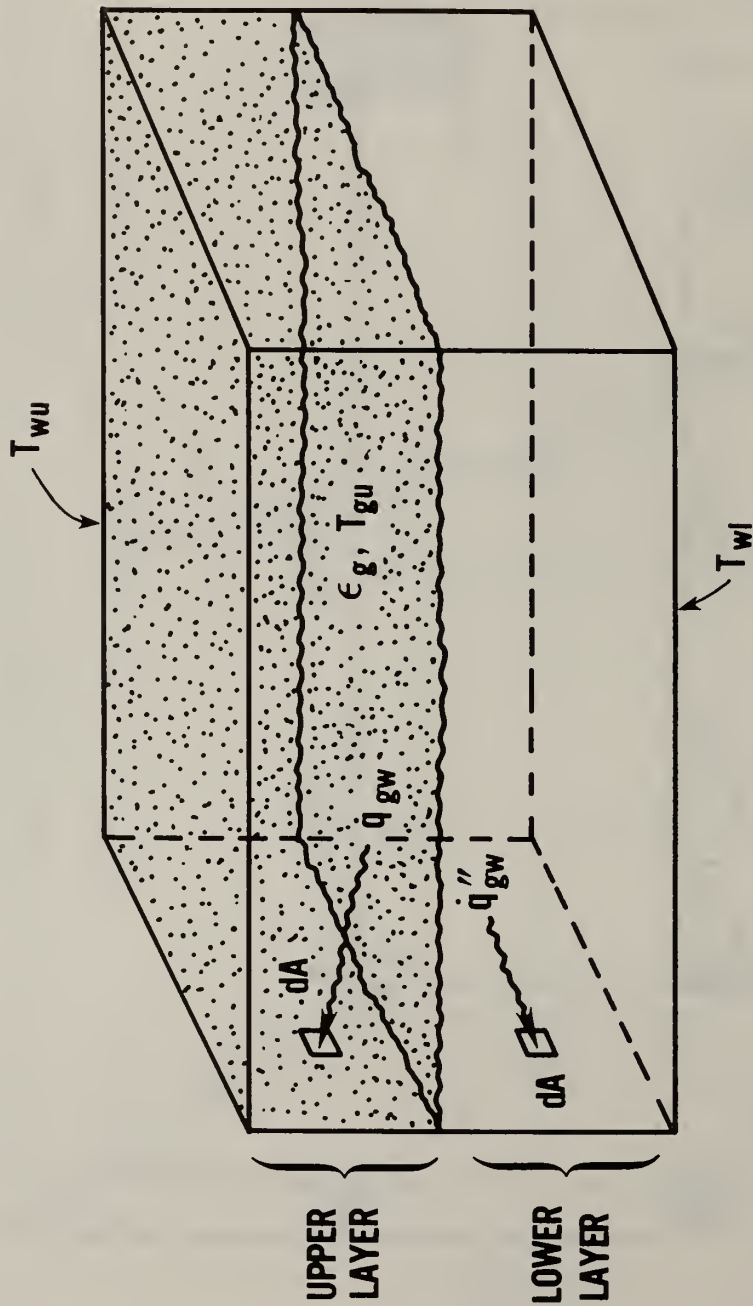
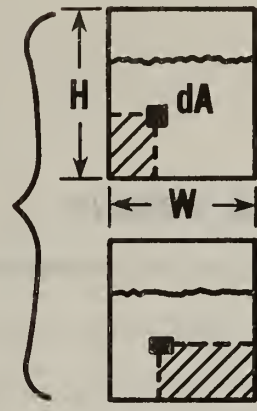$$\dot{q}''_{gw} = \dot{q}''(\text{upper gas}) + \dot{q}''(\text{upper surfaces}) + \dot{q}''(\text{lower surfaces})$$

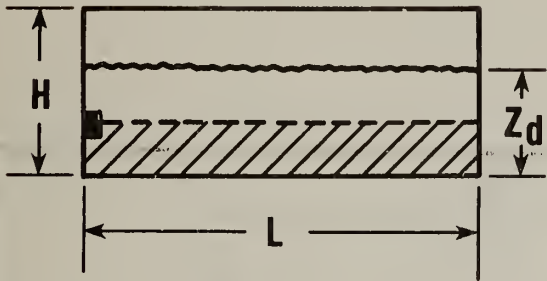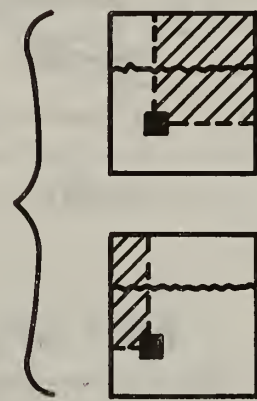Figure 7-2. Radiation from non-burning enclosure surfaces and upper gas layer to dA
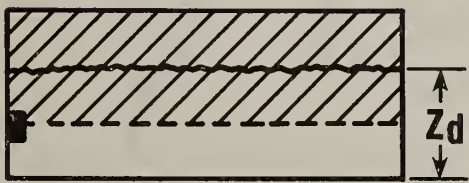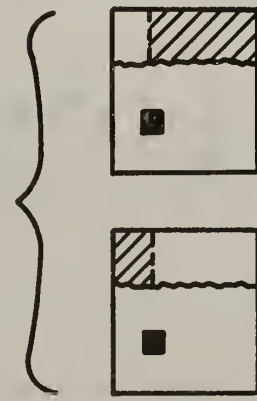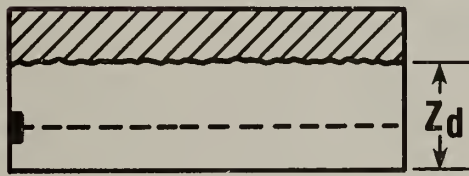
Figure 7-3. Geometrical factor for radiation from non-burning enclosure
surfaces and upper gas layer

Flaming wall elements

element s

element r

$\dot{q}_e''$

$d\dot{q}_f''$

Wall 1 (w=1)

w=2

$$\dot{q}_e'' = \sigma T_f^4 \left(1 - e^{-k_f \ell_f}\right) + \epsilon_s \sigma T_s^4 e^{-k_f \ell_f}$$

$$\dot{q}_f'' = \sum_{A_b} \dot{q}_e'' \, e^{-k_g \ell_g} \, F_{s,r}$$
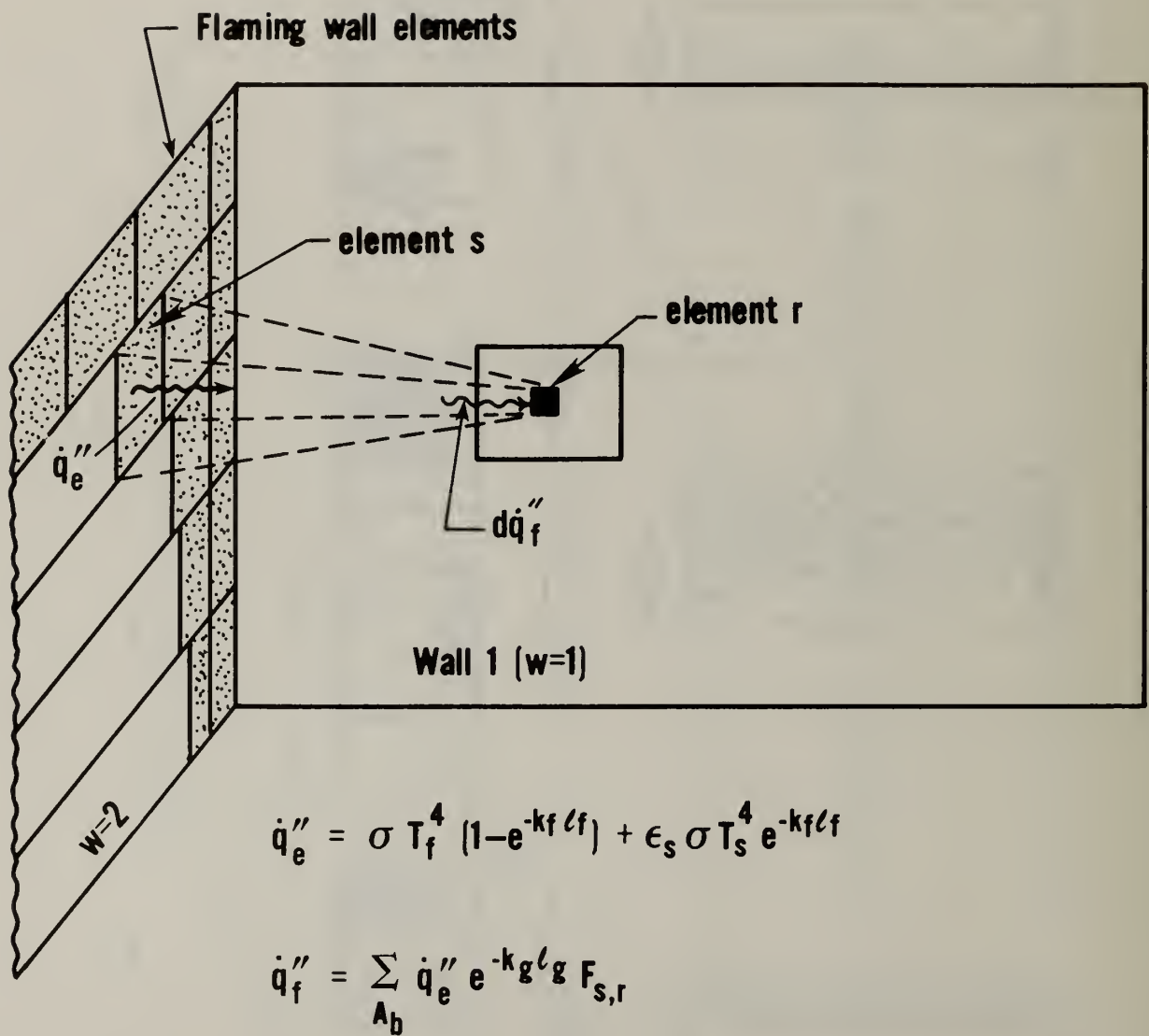
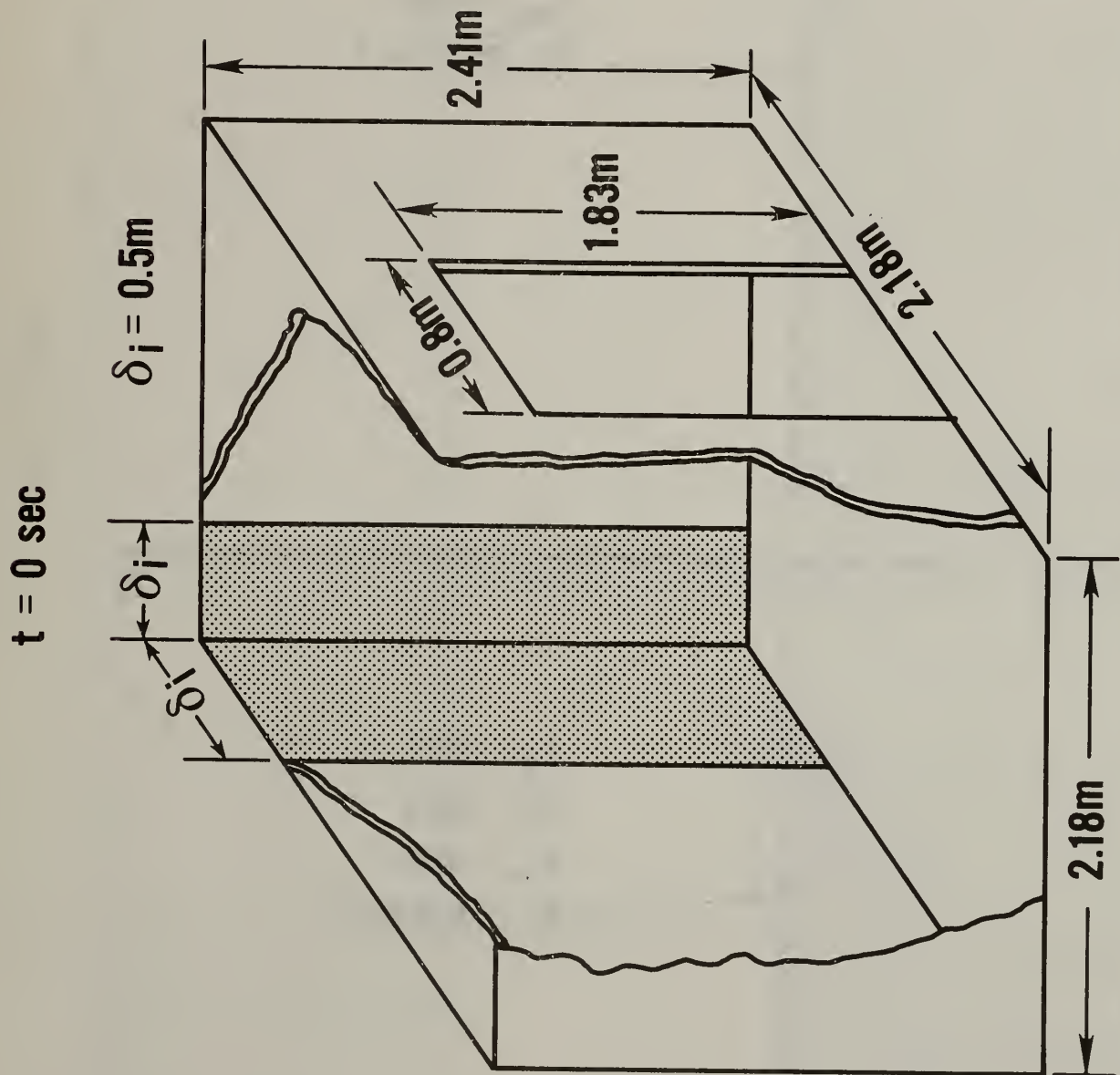Figure 7-4. Radiation from burning elements on adjacent wall

Figure 7-5. Initial area of involvement for wall spread calculations
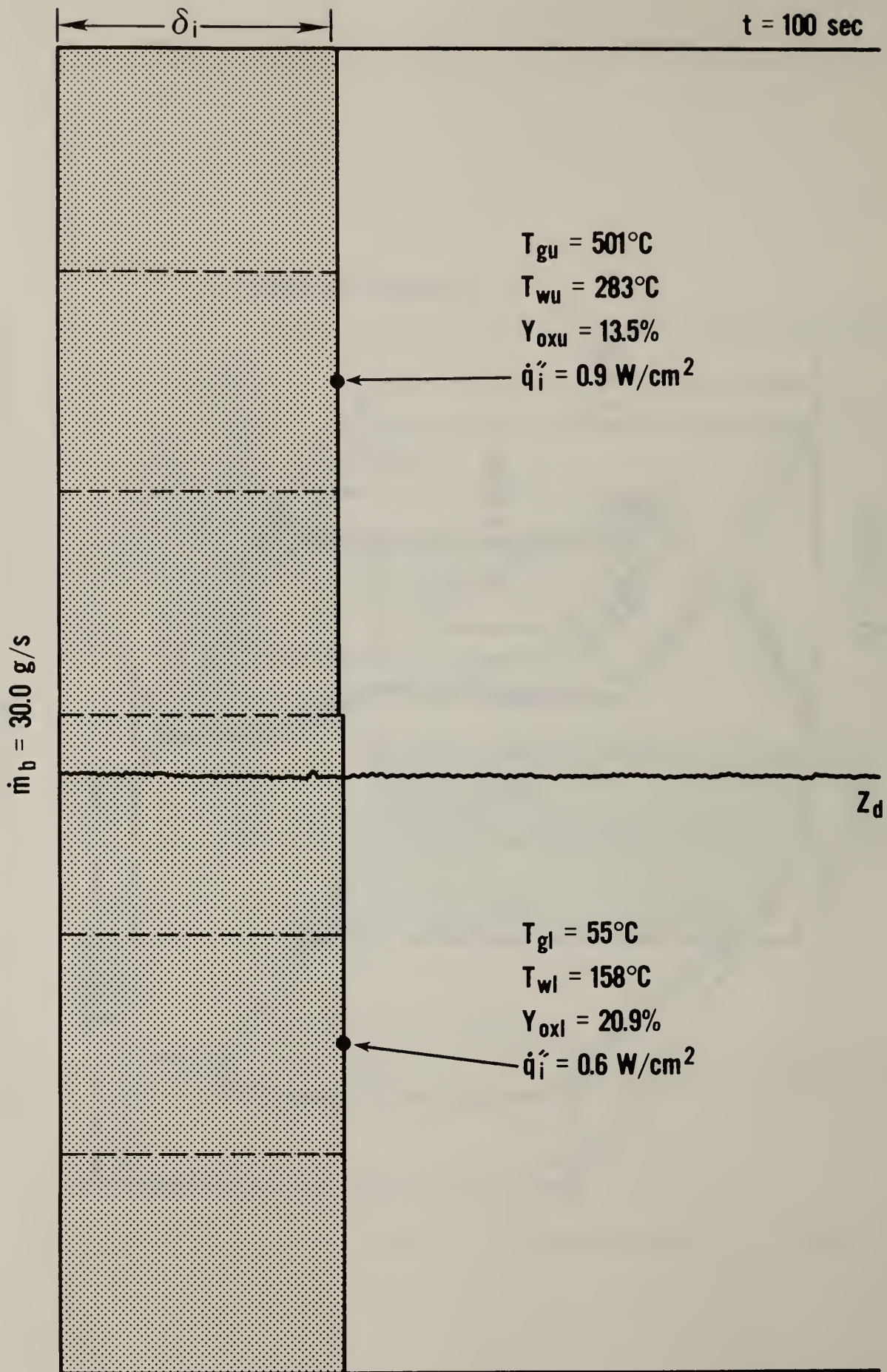
Figure 7-6. Theoretical wall spread results at t = 100 seconds
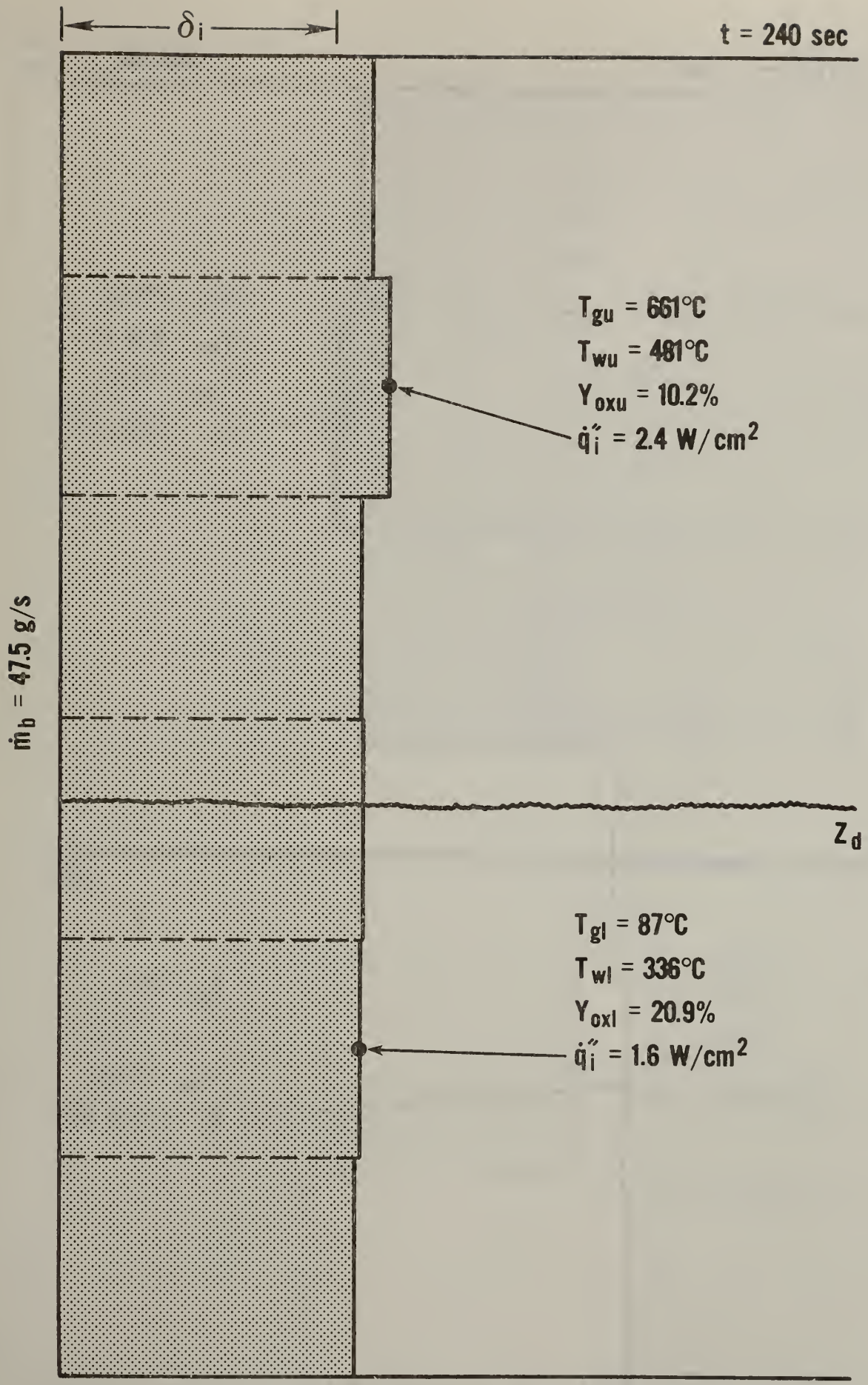
Figure 7-7. Theoretical wall spread results at t = 240 seconds
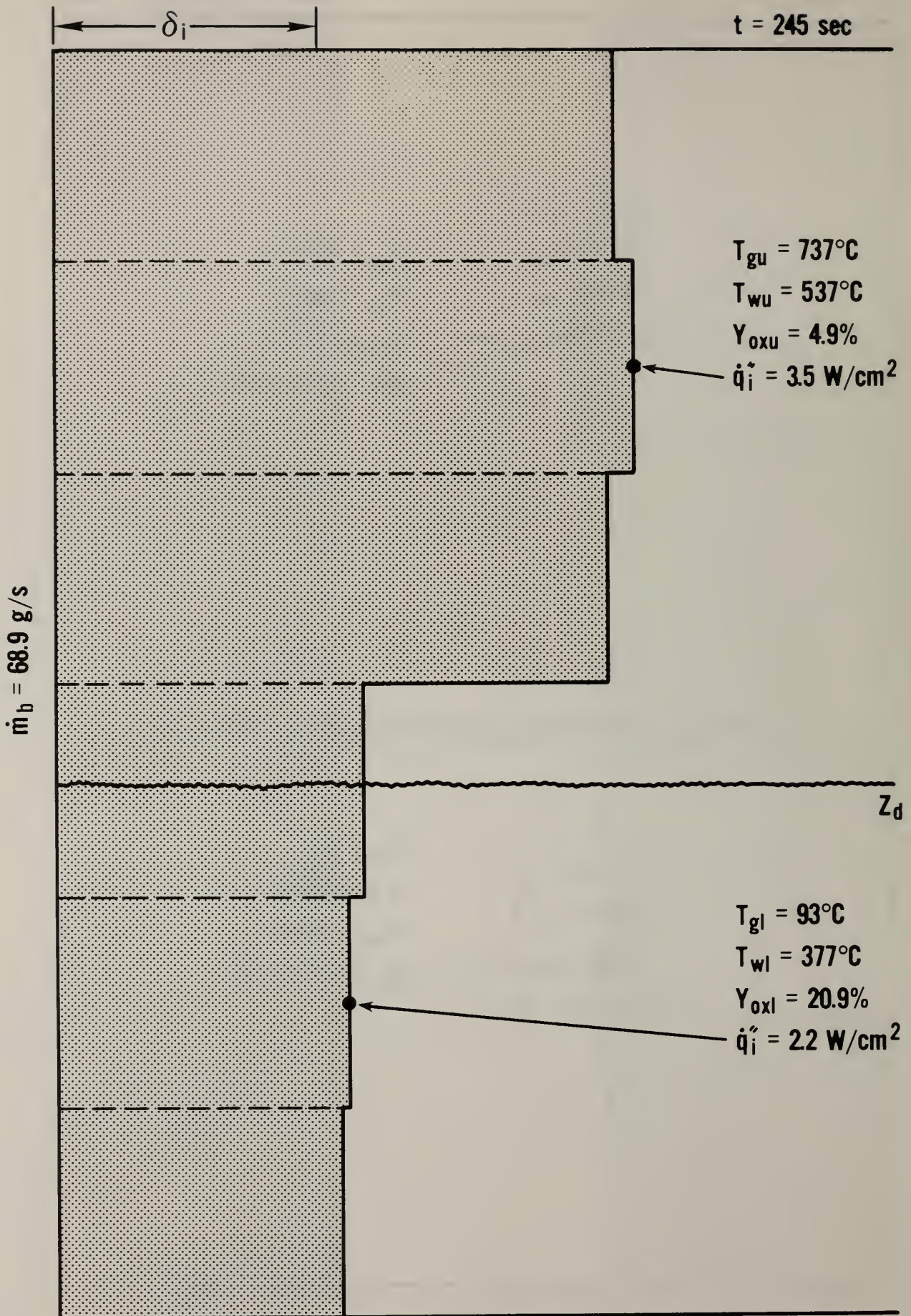
Figure 7-8. Theoretical wall spread results at t = 245 seconds
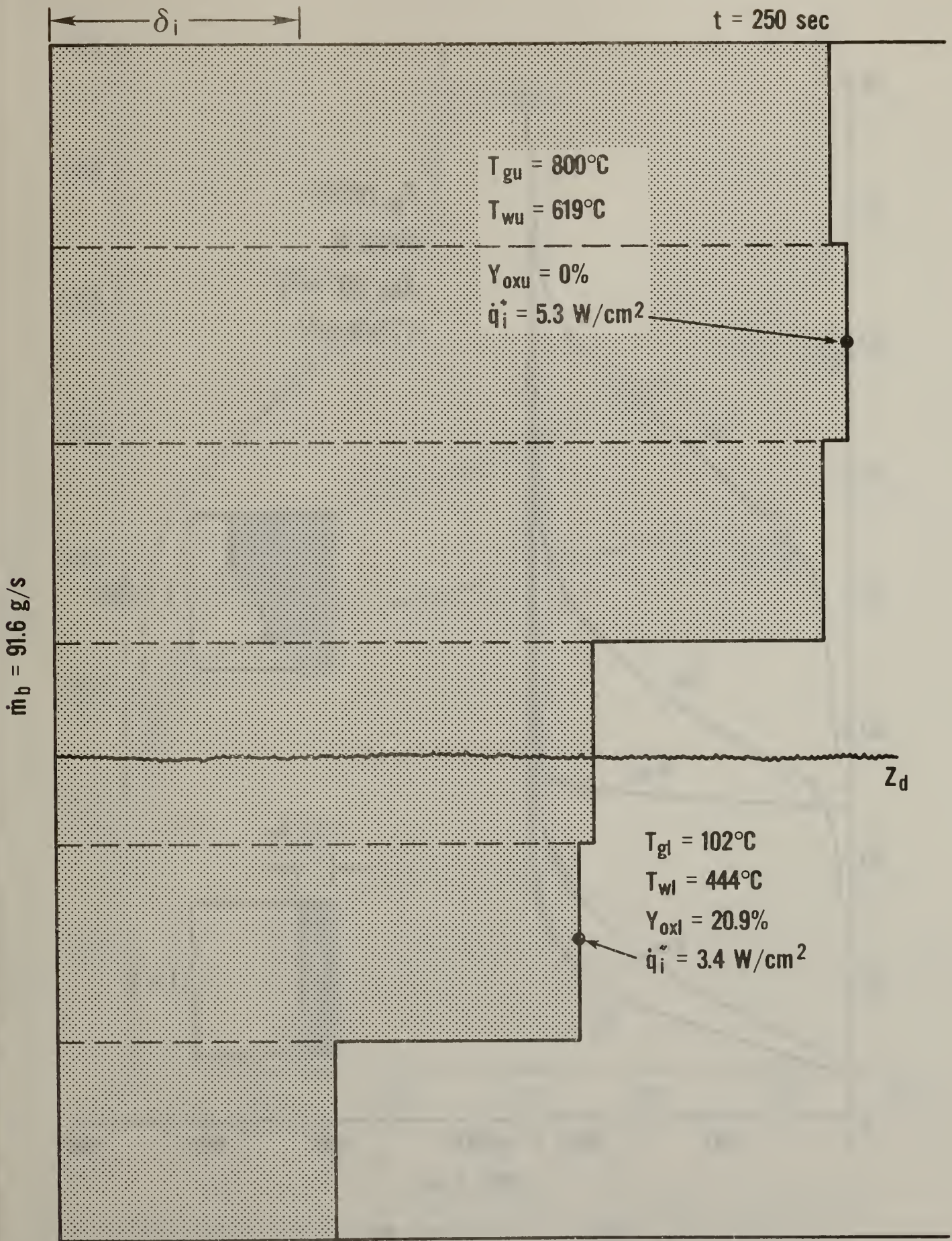
Figure 7-9.   Theoretical wall spread results at t = 250 seconds
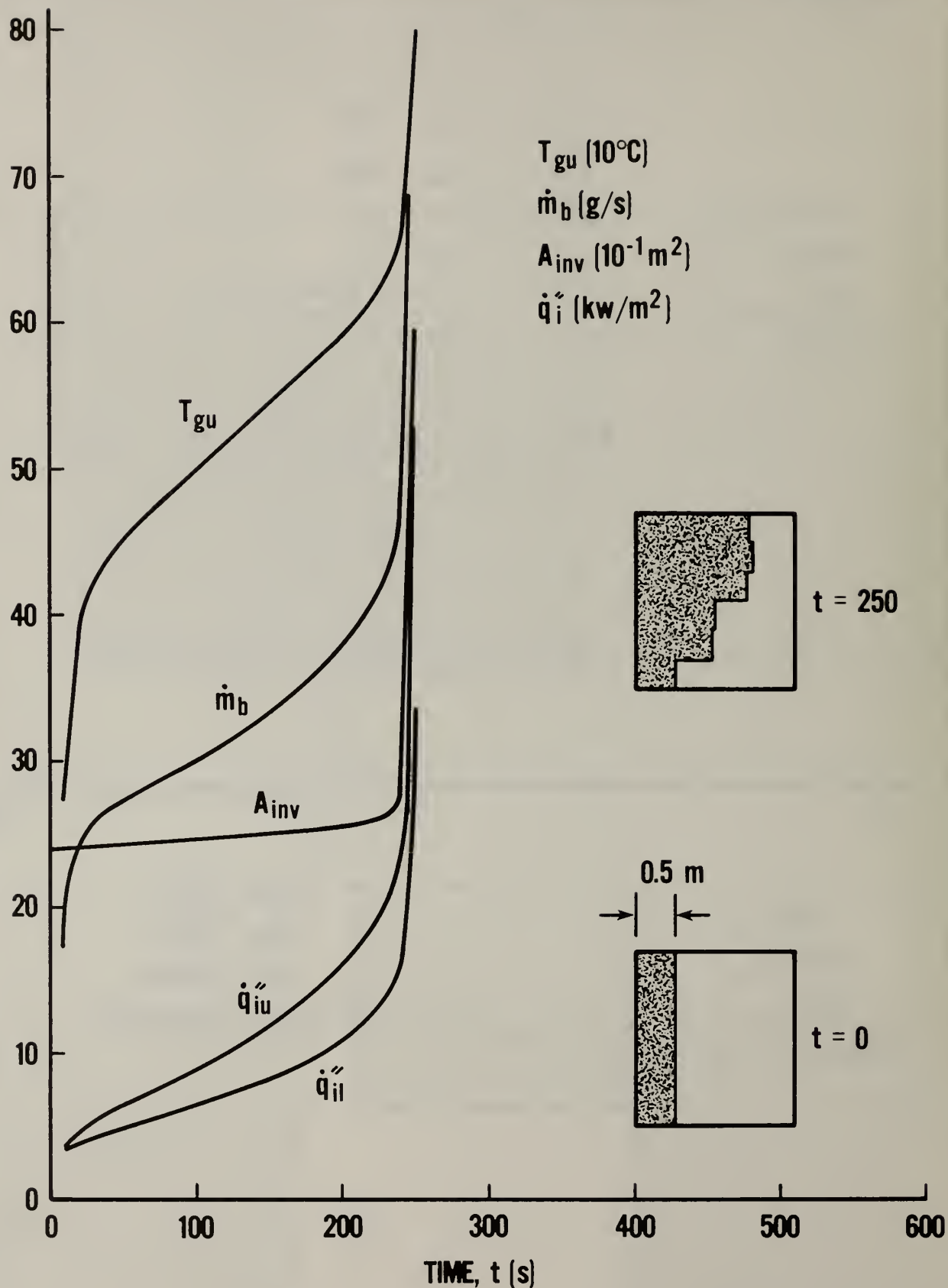
Figure 7-10. Summary of theoretical corner wall spread results:
initial burning area on each wall = 0.5m X H
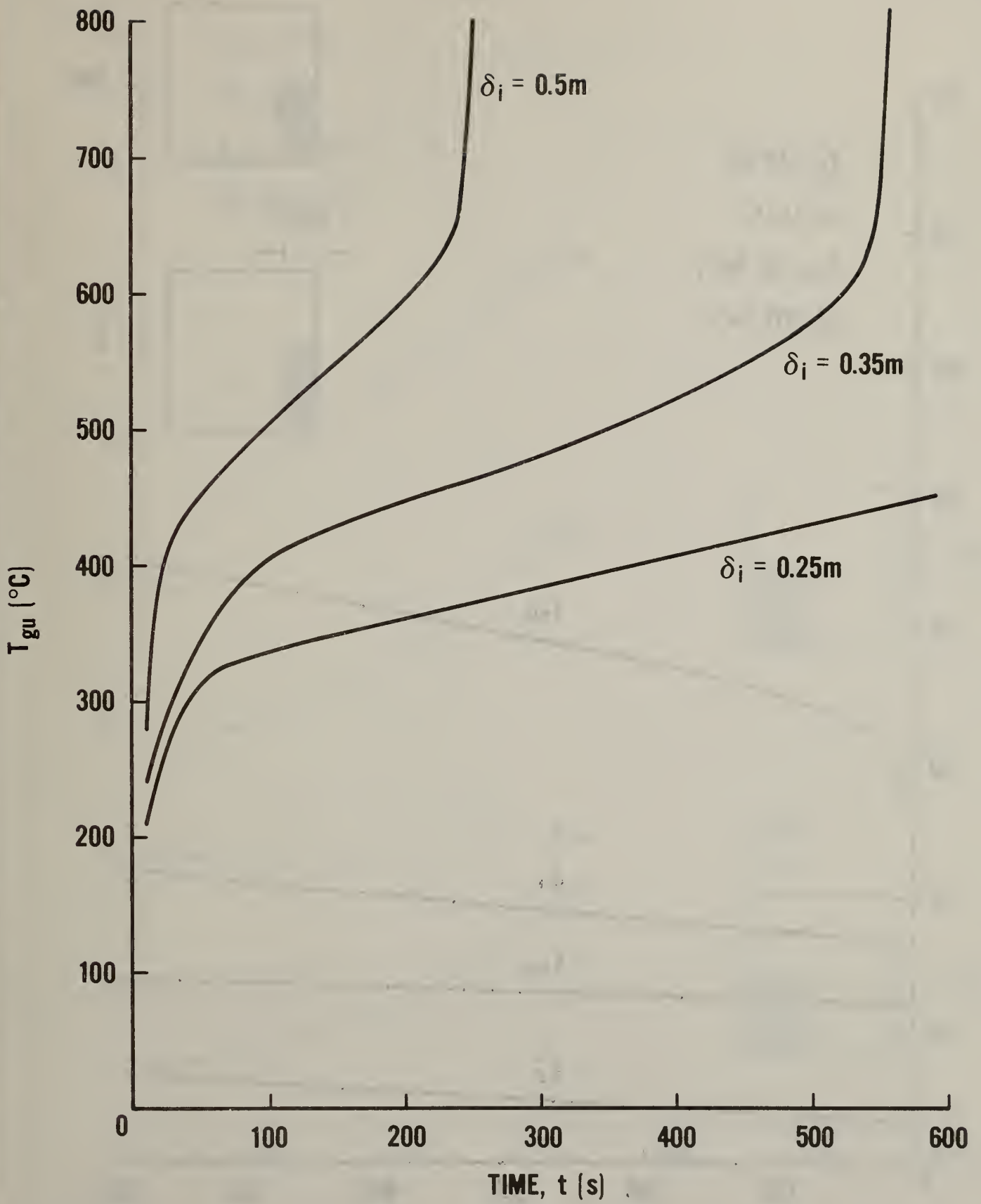
Figure 7-11. Theoretical upper gas temperatures from corner wall
spread calculations: initial burning area on each
wall = δ_i X H

Figure 7-12.   Summary of theoretical corner wall spread results:
initial burning area on each wall = 0.5m X H/2
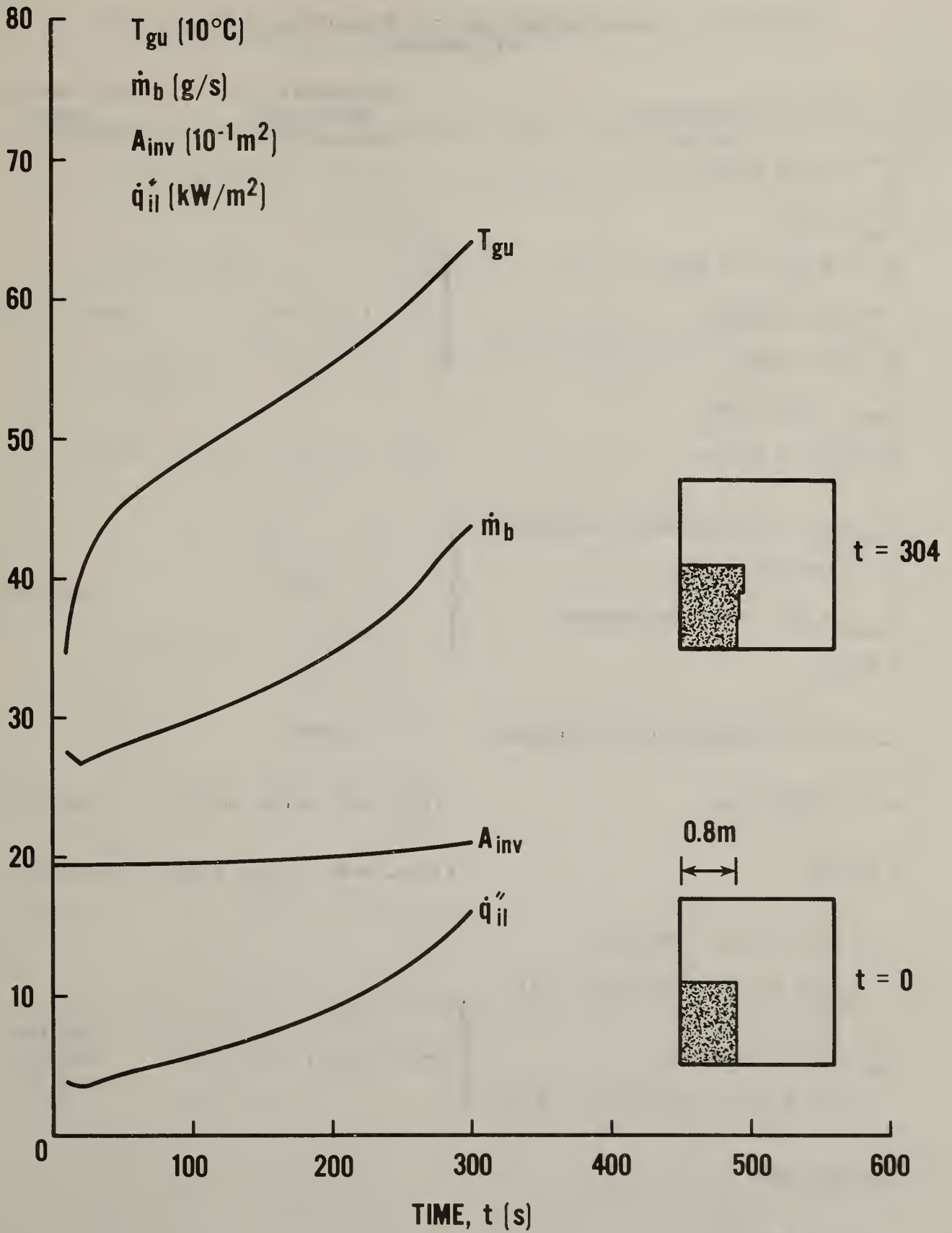
Figure 7-13. Summary of theoretical corner wall spread results:
initial burning area on each wall = 0.8m X H/2

Table 8-1. Thermophysical and Fire Properties of Hypothetical
Wall Material

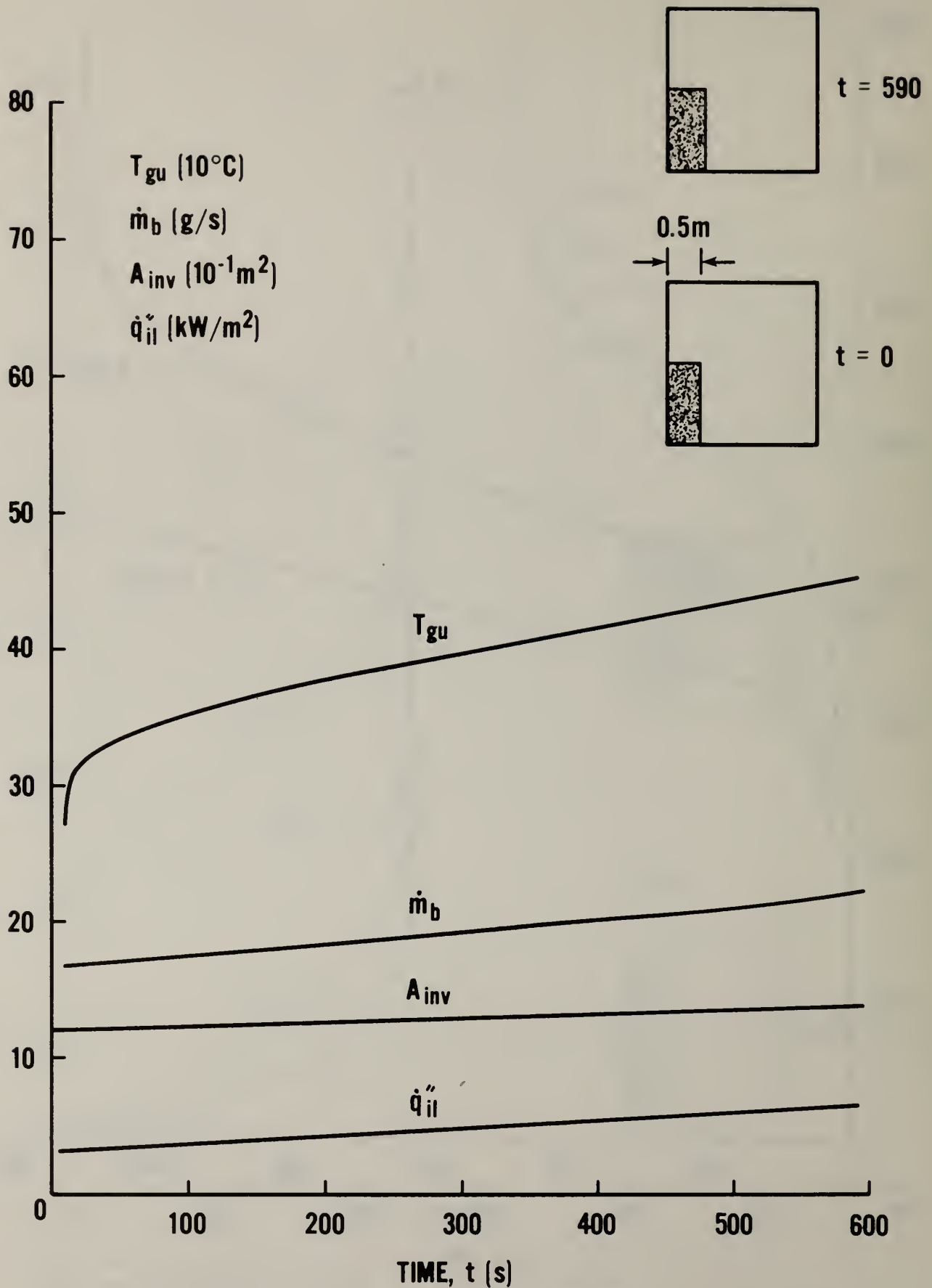| Parameter	Equation(s) in which used	Real Material basis
$\dot{m}_b^{''*} = 0.011$ kg/m^2-s		
$Y_{ox}^* = 0.233$		
$\dot{q}_i^{''*} = \sigma T_a^4 = 0.4$ kW/m^2		
$\xi = 0.108$ kg/m^2-s	(7-1, 7-2)	PMMA [15, 21]
$\dot{q}_i^{''**} = 11$ kW/m^2		
$L_{vap} = 1620$ kJ/kg		
$\dot{m}_{b;crit}^{''} = 5$ g/m^2-s		
$Y_{ox,crit} = 0$ (arbitrarily selected)		
$C = 5.06$ m$^{3/2}$s$^{1/2}$/kW		
$\dot{q}_{i,ig}^{''} = 22.4$ kW/m^2 (estimated)	(7-7)	PMMA [22]
$m = 2$		
$v_\infty = 0.1$ m/s (arbitrarily selected)	(7-9)	
$\Delta H = 15000$ kJ/kg	(A-3, A-5, A-11c, A-17)	Wood [12]
$r = 4.92$	(A-3a, A-8d, A-11b, A-19)	Wood [12]
$k_w = (0.125 \times 10^{-3}$ kW/m-K) $\cdot$ $[1 + 6.7 \times 10^{-4} K^{-1}(T_w - T_a)]$		
$c_{pw} = (1.12$ kJ/kg-K) $\cdot$ $[1 + 6.7 \times 10^{-4} K^{-1}(T_w - T_a)]$	(4-8 to 4-11, 4-13, 4-15)	Calcium Silicate Board [12]
$\rho_w = 696$ kg/m^3		
$\delta_w = 1.59 \times 10^{-2}$ m		

Appendix A - Subsidiary Equations

All subsidiary equations are functions of input parameters and/or one or more of the seven independent variables - Z_n, Z_d, T_{gu}, T_{gl}, T_{wu}, T_{wl}, $\dot{m}_v$.

$$\dot{m}_o = \frac{2}{3} W_o \, \rho_a \, C_o \sqrt{2g \frac{T_a}{T_{gu}} \left(1 - \frac{T_a}{T_{gu}}\right)} \cdot (H_o - Z_n)^{3/2} \tag{A-1}$$

$$\dot{m}_i = \frac{2}{3} W_o \, \rho_a \, C_i \, \sqrt{2g} \cdot \left[a^{1/2}(Z_n - Z_d) + \frac{(a + b \, Z_d)^{3/2} - a^{3/2}}{b} \right] \tag{A-2}$$

$$\text{where} \quad a = \left(1 - \frac{T_a}{T_{gu}}\right) (Z_n - Z_d) \tag{A-2a}$$

$$b = 1 - \frac{T_a}{T_{gl}} \tag{A-2b}$$

$$\dot{m}_p = \begin{cases} 8 \, \dot{m}_b + 0.055 \, \dot{m}_b \, \Delta H \, (Z_d - H_c) \\ \qquad\qquad \text{when } Z_d \geq H_c \\ 8 \, \dot{m}_b \qquad \text{when } Z_d \leq H_c \end{cases} \tag{A-3}$$

$$\text{where} \quad \dot{m}_b = \begin{cases} \dot{m}_v \; ; \; r \leq \dot{m}_i / \dot{m}_v \\ \dfrac{\dot{m}_i}{r} \; ; \; r > \dot{m}_i / \dot{m}_v \end{cases} \tag{A-3a}$$

$$\dot{m}_e = k_m \, \frac{T_a}{T_{gu}} \, \frac{Z_n - Z_d}{Z_n} \left(\frac{W}{W_o}\right) 0.025 \, \dot{m}_i \tag{A-4}$$

$$\dot{E}_{Ru} = \left(1 - \frac{f}{2}\right) \dot{m}_b \, \Delta H \tag{A-5}$$

$$\dot{E}_{Mu} = \left(\dot{m}_i + \dot{m}_v + \dot{m}_e\right) c_p \left(T_{gu} - T_{gl}\right) - m_v \, T_s - T_{gl} - \dot{m}_v c_{pp} \left(T_s - T_{gl}\right) \tag{A-6}$$

53

where the last term which accounts for pyrolysis gases emerging from the
surface at T_s will be neglected.

$$E_{Lu} = \left(\dot{q}''_{ru} + \dot{q}''_{cu} \right) A_{wu} + \dot{q}''_{ro} A_{ou} + \dot{q}''_{rd} A_F \tag{A-7}$$

$$\begin{aligned}\dot{q}''_{ru} = \epsilon_g \, \sigma \, T_{gu}^4 + \gamma_u \left(1 - \epsilon_g \right) \sigma \, T_{wl}^4 \\ - \left[1 - \left(1 - \gamma_u \right) \left(1 - \epsilon_g \right) \right] \sigma \, T_{wu}^4\end{aligned} \tag{A-8}$$

$$\gamma_u = \frac{A_F}{A_{wu}} \tag{A-8a}$$

$$\epsilon_g = 1 - e^{-k_g L_m} \tag{A-8b}$$

$$k_g = \frac{k_f \left(1 + X_a r \right) \dot{m}_v}{\left(\dot{m}_i + \dot{m}_v \right)} \tag{A-8c}$$

$$L_m = \frac{2WL \left(H - Z_d \right)}{\left(H - Z_d \right) \left(W + L \right) + WL} \tag{A-8d}$$

$$\dot{q}''_{ro} = \epsilon_g \, \sigma \, T_{gu}^4 + \left(1 - \epsilon_g \right) \sigma \, T_{wu}^4 - \sigma \, T_a^4 \tag{A-9}$$

$$\dot{q}''_{rd} = \epsilon_g \, \sigma \, T_{gu}^4 + \left(1 - \epsilon_g \right) \sigma \, T_{wu}^4 - \sigma \, T_{wl}^4 \tag{A-10}$$

$$\dot{q}''_{cu} = h_{cu} \left(T_{gu} - T_{wu} \right) \tag{A-11}$$

$$h_{cu} = \rho_a \, c_p \, \sqrt{gH} \; Q*^{1/3} \, C\left(\frac{r}{H} \right) \tag{A-11a}$$

$$Q* = \frac{\left(1 - f \right) \dot{m}_b \, \Delta H}{\rho_a \, c_p \, T_a \, \sqrt{gH} \; H^2} \tag{A-11b}$$

$$\dot{E}_{M1} = c_p \, \dot{m}_i \, \left(T_{g1} - T_a \right) + c_p \, \dot{m}_e \, \left(T_{g1} - T_{gu} \right) \tag{A-12}$$

$$\dot{E}_{L1} = h_{c1} \, A_{w1} \, \left(T_{g1} - T_{w1} \right) \tag{A-13}$$

$$\dot{q}''_{ku} = \frac{2}{\sqrt{\pi}} \sqrt{\frac{(k \, \rho \, c_p)_{wall}}{t^*}} \, \left(T_{wu} - T_a \right) \tag{A-14}$$

$$\dot{q}''_{k1} = \frac{2}{\sqrt{\pi}} \sqrt{\frac{(k \, \rho \, c_p)_{wall}}{t^*}} \, \left(T_{w1} - T_a \right) \tag{A-15}$$

$$\dot{q}''_{c1} = h_{c1} \left(T_{g1} - T_{w1} \right) \tag{A-16}$$

$$\dot{q}''_{r1} = \gamma_1 \, \varepsilon_g \, \sigma \, T_{gu}^4 + \left(1 - \varepsilon_g \right) \sigma \, T_{wu}^4 - \sigma \, T_{w1}^4 + \frac{f}{2} \, \frac{\dot{m}_b \, \Delta H}{A_{w1}} \tag{A-17}$$

$$\gamma_1 = A_F / A_{w1} \tag{A-17a}$$

$$Y_{ox1} = \frac{0.23 + \left(\dot{m}_e / \dot{m}_i \right) Y_{oxu}}{1 + \left(\dot{m}_e / \dot{m}_i \right)} \tag{A-18}$$

$$Y_{oxu} = \frac{0.23 \cdot \left[1 - r \left(\dot{m}_b / \dot{m}_i \right) \right]}{1 + \left(\dot{m}_v / \dot{m}_i \right)} \tag{A-19}$$

Appendix B - Radiation from Upper Gas Layer and

Non-Burning Enclosure Surfaces

A. Target Element in Lower Layer

Using Figure B-1 and following Siegel and Howell [18], the incident radiative flux on a target element in the lower layer due to radiation from the upper gas layer and enclosure surfaces is given by the expression

$$
\begin{aligned}
\dot{q}''_{gw} = F_{dA,1} \ \sigma \ T^4_{wl} + F_{dA,2} \ \sigma \ T^4_{wl} & \quad \text{radiation from quadrants} \\
& \quad \text{i=1 and i=2}
\end{aligned}
$$

$$
\begin{rcases}
+ \ F_{dA,5} \left[\sigma\epsilon_{g,5} \ T^4_{gu} + \left(1-\epsilon_{g,5}\right) \ \sigma \ T^4_{wu} \right] \\[2em]
+ \ F_{dA,6} \left[\sigma\epsilon_{g,6} \ T^4_{gu} + \left(1-\epsilon_{g,6}\right) \ \sigma \ T^4_{wu} \right]
\end{rcases}
\begin{aligned}
& \text{radiation from gas} \\
& \text{and upper surfaces in} \\
& \text{quadrants i=3 and i=4}
\end{aligned}
$$

$$
\begin{rcases}
+ \left(F_{dA,3} - F_{dA,5}\right) \ \sigma \ T^4_{wl} \\[2em]
+ \left(F_{dA,4} - F_{dA,6}\right) \ \sigma \ T^4_{wl}
\end{rcases}
\begin{aligned}
& \text{radiation from lower} \\
& \text{surfaces in quadrants} \\
& \text{i=3 and i=4}
\end{aligned}
$$

$$\tag{B-1}$$

or

$$
\dot{q}''_{gw} = \sum_{i=1}^{4} \ \sigma \ F_{dA,i} \ T^4_{wl} + \sum_{i=5}^{6} \ \sigma \ F_{dA,i} \left[\epsilon_{g,i} \ T^4_{gu} + \left(1-\epsilon_{g,i}\right) \ T^4_{wu} - T^4_{wl} \right] \tag{B-2}
$$

where $F_{dA,1} = F_{dA,2} = F_{dA,3} = F_{dA,4} = 0.25$ $\hspace{2cm}$ (B-3)

$$
F_{dA,5} = F_{dA,3} - F_{dA,I} \left(\frac{x}{L} , \frac{|z_d-z|}{L} \right) - F_{dA,II} \left(\frac{L}{|z_d-z|} , \frac{L}{|z_d-z|} \right) \tag{B-4}
$$

$$
F_{dA,6} = F_{dA,4} - F_{dA,I} \left(\frac{W-x}{L} , \frac{|z_d-z|}{L} \right) - F_{dA,II} \left(\frac{W-x}{|z_d-z|} \right) \tag{B-5}
$$

and [16]

$$F_{dA,I}(X,Y) = \frac{1}{2\pi}\left[\frac{X}{\sqrt{1+X^2}}\tan^{-1}\frac{Y}{\sqrt{1+X^2}} + \frac{Y}{\sqrt{1+Y^2}}\tan^{-1}\frac{X}{\sqrt{1+Y^2}}\right] \quad (B\text{-}6)$$

$$F_{dA,II}(X,Y) = \frac{1}{2\pi}\left(\tan^{-1}\frac{1}{Y} - AY\tan^{-1}A\right) \quad (B\text{-}7)$$

$$\text{where } A = 1/\sqrt{X^2 + Y^2} \quad (B\text{-}7a)$$

B. **Target Element in Upper Layer**

Using Figure B-2 and following Siegel and Howell [18]

$$\dot{q}''_{gw} = F_{dA,1}\left[\varepsilon_{g,1}\,\sigma\,T_{gu}^4 + (1-\varepsilon_{g,1})\,\sigma\,T_{wu}^4\right] \left.\begin{array}{c}\\\\\end{array}\right\} \quad \text{radiation from quadrants } i=1 \text{ and } i=2$$

$$+ F_{dA,2}\left[\varepsilon_{g,2}\,\sigma\,T_{gu}^4 + (1-\varepsilon_{g,2})\,\sigma\,T_{wu}^4\right]$$

$$+ F_{dA,5}\,(1-\varepsilon_{g,5})\,\sigma\,T_{wl}^4 \qquad\qquad\qquad \text{radiation from lower surfaces of quadrants } i=3 \text{ and } i=4$$

$$+ F_{dA,6}\,(1-\varepsilon_{g,5})\,\sigma\,T_{wl}^4$$

$$+ F_{dA,3}\,\varepsilon_{g,3}\,\sigma\,T_{gu}^4 + (F_{dA,3} - F_{dA,5})$$

$$\cdot\,(1-\varepsilon_{g,3})\,\sigma\,T_{wu}^4 \qquad\qquad\qquad \text{radiation from gas and upper surfaces in quadrants } i=3 \text{ and } i=4$$

$$+ F_{dA,4}\,\varepsilon_{g,4}\,\sigma T_{gu}^4 + (F_{dA,4} - F_{dA,6})$$

$$\cdot\,(1-\varepsilon_{g,4})\,\sigma T_{wu}^4 \qquad\qquad\qquad\qquad (B\text{-}8)$$

or

$$\dot{q}''_{gw} = \sum_{i=1}^{4} \sigma F_{dA,i} \left[\epsilon_{g,i} T_{gu}^4 + (1-\epsilon_{g,i}) T_{wu}^4 \right]$$

$$+ \sum_{i=5}^{6} \sigma F_{dA,i} (1-\epsilon_{g,i}) \left(T_{wl}^4 - T_{wu}^4 \right)$$

(B-9)

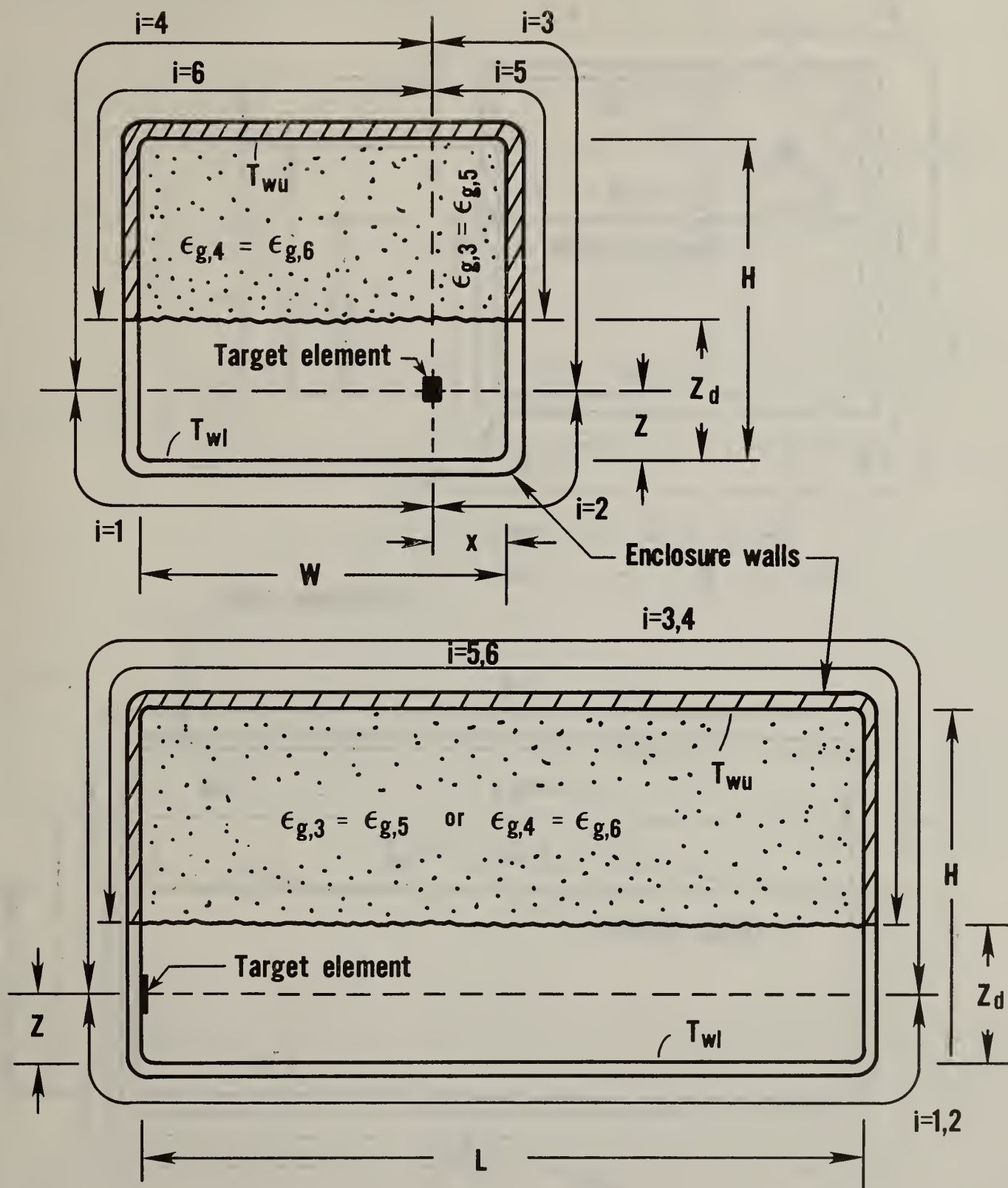where the geometrical factors are defined by equations B-3 to B-7.

58

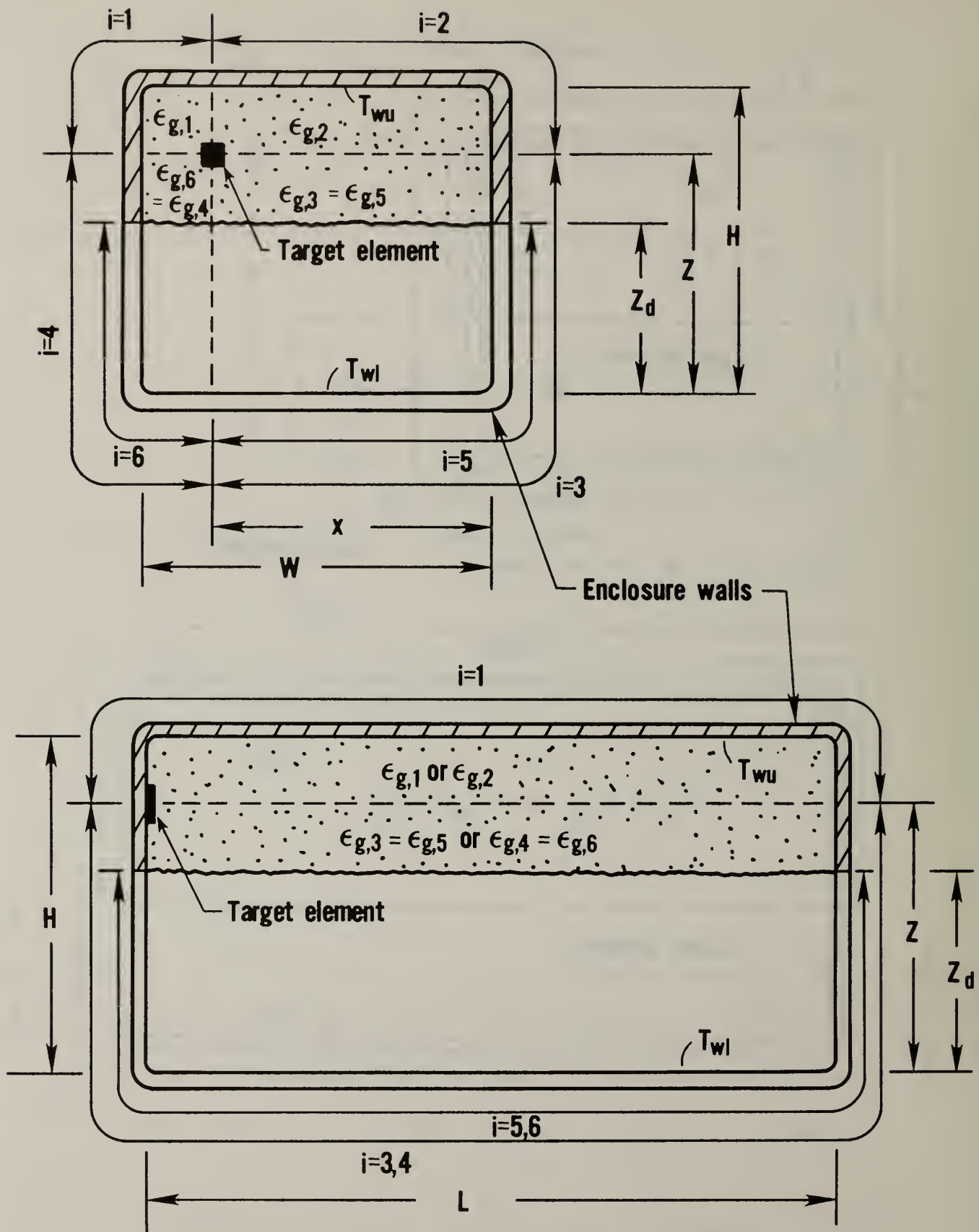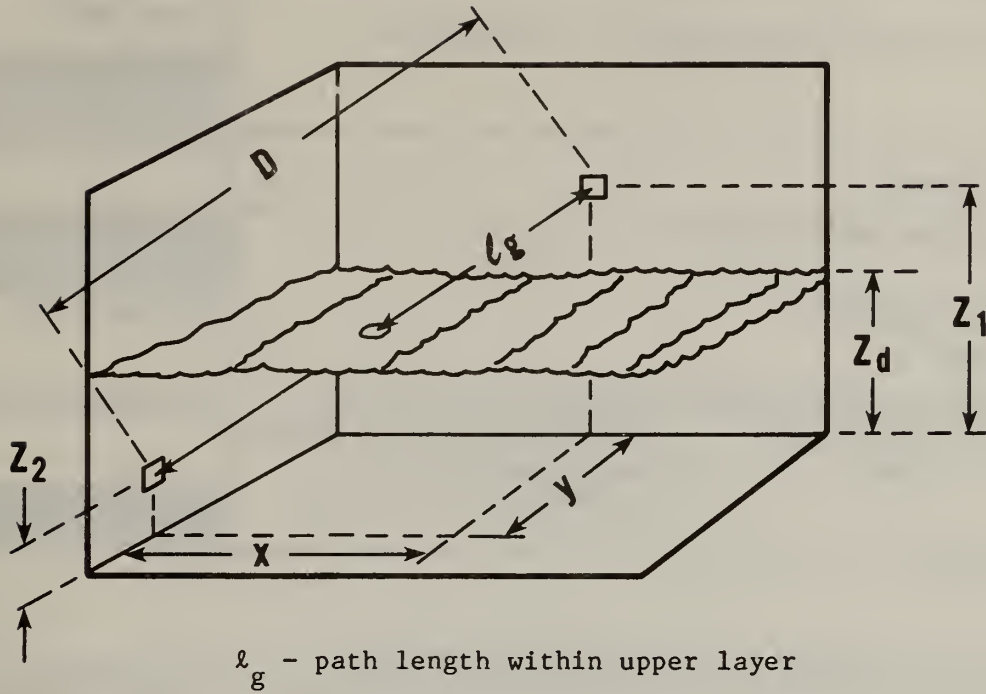Figure B-1. Radiation target element in lower layer

Figure B-2. Radiation target element in upper layer

Appendix C - Radiation Path Length Through Upper Layer

ℓ_g - path length within upper layer

$$D = \sqrt{x^2 + y^2 + (z_1 - z_2)^2} \qquad (C-1)$$

when

$$z_1 = z_2 \quad \left\{ \begin{array}{l} z_2 \geq z_d; \; \ell_g = D \\[2ex] z_2 < z_d; \; \ell_g = 0 \end{array} \right. \qquad (C-2)$$

$$z_1 \neq z_2 \left\{ \begin{array}{ll} z_1 \geq z_d & \left\{ \begin{array}{l} z_2 \geq z_d; \; \ell_g = D \\[2ex] z_2 < z_d; \; \ell_g = \dfrac{z_1 - z_d}{z_1 - z_2} \, D \end{array} \right. \\[5ex] z_1 = z_d & \left\{ \begin{array}{l} z_2 \geq z_d; \; \ell_g = D \\[2ex] z_2 < z_d; \; \ell_g = 0 \end{array} \right. \\[5ex] z_1 < z_d & \left\{ \begin{array}{l} z_2 \leq z_d; \; \ell_g = 0 \\[2ex] z_2 > z_d; \; \ell_g = \dfrac{z_2 - z_d}{z_2 - z_1} \, D \end{array} \right. \end{array} \right. \qquad (C-3)$$

U.S. DEPT. OF COMM. BIBLIOGRAPHIC DATA SHEET	1. PUBLICATION OR REPORT NO. NBSIR-83-2765	2. Gov't. Accession No.	3. Recipient's Accession No.

4. TITLE AND SUBTITLE

A Calculation of Wall Fire Spread in an Enclosure

5. Publication Date
Nov 1983

6. Performing Organization Code

7. AUTHOR(S)
Kenneth D. Steckler

8. Performing Organ. Report No.

9. PERFORMING ORGANIZATION NAME AND ADDRESS

NATIONAL BUREAU OF STANDARDS
DEPARTMENT OF COMMERCE
WASHINGTON, DC 20234

10. Project/Task/Work Unit No.

11. Contract/Grant No.

12. SPONSORING ORGANIZATION NAME AND COMPLETE ADDRESS *(Street, City, State, ZIP)*

Armstrong World Industries   U.S. Department of Health
Lancaster, PA 17604   and and Human Services
                Washington, D.C. 20201

13. Type of Report & Period Covered

14. Sponsoring Agency Code

15. SUPPLEMENTARY NOTES

☐ Document describes a computer program; SF-185, FIPS Software Summary, is attached.

16. ABSTRACT *(A 200-word or less factual summary of most significant information. If document includes a significant bibliography or literature survey, mention it here.)*

Mathematical models of fire growth in enclosures offer a potential for assessing the risk of materials with respect to a hazard such as flashover. The development of a model for fire spread over wall lining materials is presented. The work covers the development of a transient two-layer zone model, initially formulated for crib fires in a room, then adapted to simulate a spreading corner wall fire. The local wall flame spread rate and burning rate per unit area are expressed in the model as functions of the external radiation incident upon the burning surface and the oxygen concentration in the adjacent gas layer (zone). Flame spread is limited to the horizontal direction. Results for a fictitious wall lining material are presented. Major elements of the results are shown to be in qualitative agreement with experience. Finally, areas for improvement and the direction of future efforts are noted.

17. KEY WORDS *(six to twelve entries; alphabetical order; capitalize only the first letter of the first key word unless a proper name; separated by semicolons)*

burning rate; fire models; flame spread; flashover; mathematical models; room fires; walls

18. AVAILABILITY ☒ Unlimited	19. SECURITY CLASS (THIS REPORT)	21. NO. OF PRINTED PAGES
☐ For Official Distribution. Do Not Release to NTIS	UNCLASSIFIED	74
☐ Order From Sup. of Doc., U.S. Government Printing Office, Washington, DC 20402, SD Stock No. SN003-003-	20. SECURITY CLASS (THIS PAGE)	22. Price
☒ Order From National Technical Information Service (NTIS), Springfield, VA. 22161	UNCLASSIFIED	